Les Cahiers du GERAD ISSN: 0711–2440

The impact of synchronizing driver breaks and recharging operations for electric vehicles

M. Schiffer, G. Laporte
M. Schneider, G. Walther

G–2017–46

June 2017

GERAD HEC Montréal
3000, chemin de la Côte-Sainte-Catherine
Montréal (Québec) Canada H3T 2A7

Tél. : 514 340-6053
Téléc. : 514 340-5665
info@gerad.ca
www.gerad.ca

The impact of synchronizing driver breaks and recharging operations for electric vehicles

Maximilian Schiffer [a]
Gilbert Laporte [b]
Michael Schneider [c]
Grit Walther [a]

[a] *RWTH Aachen University, School of Business and Economics, Chair of Operations Management, 52072 Aachen, Germany*

[b] *GERAD, CIRRELT and Canada Research Chair in Distribution Management, HEC Montréal, Montréal, Canada H3T 2A7*

[c] *RWTH Aachen University, School of Business and Economics, Deutsche Post Chair of Optimization of Distribution Networks, 52072 Aachen, Germany*

maximilian.schiffer@om.rwth-aachen.de
gilbert.laporte@cirrelt.ca
michael.schneider@dpor.rwth-aachen.de
walther@om.rwth-aachen.de

June 2017

Les Cahiers du GERAD
G–2017–46

Abstract: Electric commercial vehicles (ECVs) are gaining importance as they are seen to provide a sustainable mean of transportation. However, practitioners still see ECVs as less competitive compared with internal combustion engine vehicles (ICEVs), especially in mid-haul operations where ECVs have to be recharged en route. In this paper we study the influence of hours of service (HOS) regulations on operational planning tasks of ECVs and ICEVs in mid-haul transportation. We introduce the electric vehicle routing problem with truck driver scheduling and present a mixed integer program as well as an adaptive large neighborhood search for the solution of large-size instances. We first compare the competitiveness of ECVs against ICEVs for the current state of the art in mid-haul transportation without considering HOS regulation, before we secondly analyze the impact of EU respective US HOS regulations on route patterns and costs of both vehicle types. We show, that HOS regulations affect the competitiveness of both ECVs and ICEVs and prove that synchronizing recharging and driver breaks helps to increase the competitiveness of ECVs. Cost savings of up to 20% can be achieved if ECVs are used instead of ICEVs.

Keywords: Electric vehicle routing, hours of service regulations, adaptive large neighborhood search

Acknowledgments: Gilbert Laporte was partially funded by the Canadian Natural Sciences and Engineering Research Council under grant 2015-06189. This support is gratefully acknowledged.

1 Introduction

Electric commercial vehicles (ECVs) are sustainable and environmentally friendly means of transportation that can contribute significantly to the reduction of noise, greenhouse-gas, and noxious emissions. Nevertheless, the market penetration of ECVs is still very low, although a faster uptake was envisioned by experts and politicians (Pelletier et al., 2017). Commercial logistics fleets provide an opportunity to accelerate this market penetration. ECVs can only become more attractive for high utilization rates and daily traveled distances (Feng and Figliozzi, 2013), since acquisition costs are high and operational costs are low (cf. Davis and Figliozzi, 2013). Thus, logistics fleets favor the use of ECVs due to a high utilization compared with private cars. However, their limited range and long recharging times remain as the main obstacles to a faster adoption (Pelletier et al., 2017). Because even quick recharging takes a minimum of 20 to 30 minutes, ECVs are less time-efficient than internal combustion engine vehicles (ICEVs) as soon as en route recharging operations are required, as is the case in mid and long-haul transportation. Currently, this leads to the perception that ECVs can only be used beneficially within short-haul transportation. A representative of our main industry partner, the Deutsche Post DHL group, states that using electric vehicles not only for short-haul collection and distribution but also for mid and long-haul consolidated transportation may be one of the biggest challenges to pave the way for sustainable logistics systems.

The reluctance of practitioners to use ECVs within mid and long-haul transportation is mainly backed by aggregated cost analyses that account for fixed amounts of extra time when estimating the cost of recharging. These analyses assume that idle times for recharging directly reduce the effective driving times of ECVs compared to those of ICEVs. Because driver wages are one of the dominating cost factors in transportation (Bektaş and Laporte, 2011), fleet operators are not willing to accept additional times for recharging ECVs en route. However, these aggregate analyses neglect important aspects and synergies resulting from the integration of ECVs at operational planning level. For example, ECVs may become more competitive if idle times resulting from driver breaks and customer time windows (both are identical for ECVs and ICEVs) can be synchronized with the recharging process. Such effects are not taken into account at an aggregated cost level. The only available study backing these cost analyses by operational and strategic planning results was presented by Schiffer et al. (2016) for a specific application case. However, idle times due to driver breaks were still neglected in this study. Focusing on the synchronization between idle times and recharging times, we note that it strongly depends on parameters of the transportation planning problem at hand. For this reason, the recharging schedule has to be explicitly determined at the operational level, considering working shifts and hours of service (HOS) regulations for drivers in the context of a vehicle routing problem (VRP). Therefore, more detailed analyses have to be carried out regarding the integration of ECVs at operational level.

Because HOS regulations are country-specific and differ significantly with respect to the statutory minimum durations of breaks or the times after which a break has to take place, we summarize the HOS regulations considered in this paper in Section 1.1. We then briefly review the literature on electric VRPs (EVRPs) in Section 1.2 and on truck driver scheduling problems (TDSPs) in Section 1.3, before detailing the aim and organization of our paper (Section 1.4).

1.1 European and United States HOS regulations

In this paper, we focus on the European Union (EU) and the United States (US) HOS regulations, because they represent two rather extreme cases of regulations with respect to overall driving times and required break durations. These HOS regulations are described in detail in Goel (2010) and Goel and Kok (2012) and are as follows:

European Union: In the EU, a driver must take a break of at least 45 minutes at the latest after a cumulated driving time of 4.5 hours. This break can be split into two parts, the first part being required to last at least 15 minutes, and the second at least 30 minutes. The driver can decide to take the complete break before an accumulated driving time of 4.5 hours is reached (e.g., if locations for breaks are limited). The next driving period of 4.5 hours starts at the end of the last break. Drivers are not allowed to reach an accumulated driving time larger than nine hours. However, since other activities (e.g., providing

service) are not counted as driving time, the overall duration of a daily trip may last up to 13 hours when the overall work duration is considered.

United States: In the US, a driver must take a break of at least 30 minutes after at most eight hours of accumulated driving time. In contrast to the EU HOS regulations, this break may not be split. Drivers are forced to take a rest after 11 hours of accumulated driving time or after an overall work duration of 14 hours.

1.2 Literature on the electric vehicle routing problem

The EVRP extends classical VRPs by incorporating specific characteristics of ECVs, i.e. limited driving range and battery recharging at charging stations. Conrad and Figliozzi (2011) were the first to consider a VRP with recharging operations, considering a maximum route duration for vehicles and allowing for battery recharges at certain customer locations with a fixed recharging time. Erdoğan and Miller-Hooks (2012) defined a VRP with refueling options provided by a sparse infrastructure of alternative fuel stations, and by making some simplifications, e.g., by assuming a linear energy consumption. Later publications lifted some of these simplifications and provided more effective and efficient algorithms. Some examples of extensions are customer time windows and recharging times related to the amount of energy needed (Schneider et al., 2014; Desaulniers et al., 2016; Hiermann et al., 2016), charging stations with different speeds and costs (Felipe et al., 2014; Montoya et al., 2017), the option of partial recharges (Felipe et al., 2014; Desaulniers et al., 2016; Keskin and Çatay, 2016; Montoya et al., 2017), more realistic energy consumption dependent on vehicle speed, load, and gradient (Goeke and Schneider, 2015), consideration of a heterogeneous fleet (Hiermann et al., 2016; Goeke and Schneider, 2015), and integration of EVRP into a location-routing context (Yang and Sun, 2015; Schiffer and Walther, 2017a,b; Hof et al., 2017). Most of these papers present metaheuristics, especially adaptive large neighborhood search (ALNS) which is quite popular (Goeke and Schneider, 2015; Hiermann et al., 2016; Keskin and Çatay, 2016; Schiffer and Walther, 2017a). Exact algorithms for EVRPs and electric traveling salesman problems were introduced in Desaulniers et al. (2016); Hiermann et al. (2016), and Roberti and Wen (2016). Pelletier et al. (2016) provided a survey on goods distribution using electric vehicles, while Pelletier et al. (2017) analyzed battery behavior in this context.

However, none of these contributions focuses on mid- to long-haul routing of ECVs and explicitly considers HOSs regulations. In addition, none compares the competitiveness of ECVs with respect to ICEVs based on total costs.

1.3 Literature on the truck driver scheduling problem

Recent work on truck driver scheduling can be classified into studies that exclusively focus on the scheduling of truck drivers and studies that combine truck driver scheduling with a VRP.

Focusing on the TDSP, Archetti and Savelsbergh (2009) presented a polynomial-complexity exact algorithm to sequence full truck load requests within an origin dispatch window. Goel and coauthors developed various algorithms for the TDSP in the context of different HOS regulations. More specifically, EU and US HOS regulations were studied by Goel (2012b) and extended to multiple time windows in Goel and Kok (2012). Goel and Rousseau (2012) and Goel (2012a) focused on Canadian HOS regulations. Australian HOS regulations were addressed in Goel (2012c) and Goel et al. (2012). Koç et al. (2016) introduced the TDSP with idling options (TDSPIO). These options offer different ways of keeping the vehicle at an adequate comfort level either by running the engine, by stopping at an electrified parking space, or by using an auxiliary power unit. All of these studies focus only on the scheduling aspect of break schedules according to HOS regulations and neglect the routing aspects.

Xu et al. (2003) investigated a rich pickup and delivery problem that includes several practical constraints such as multiple time windows and HOS regulations. This paper is considered to be the first publication to include HOS rules in a routing problem. Ceselli et al. (2009) studied another rich VRP in this context. Goel (2009) introduced a vehicle routing and truck driver scheduling problem (VRTDSP) that extends the VRP with time windows (VRPTW) by incorporating HOS regulations. In the VRTDSP, the schedule of

every route has to comply with a subset of the EU HOS regulations. A large neighborhood search (LNS) is presented and its performance is evaluated on a set of modified Solomon VRPTW instances. Kok et al. (2010) integrated the complete set of EU rules into the VRPTW and provided a dynamic programming (DP) heuristic to solve the problem with a planning horizon of one week. The authors tested their algorithm on the modified benchmark instances of Goel (2009) and found that slight modifications of a few rules can result in a significant improvement of the vehicle routes (and therefore of the overall costs). Prescott-Gagnon et al. (2010) studied a VRPTW with driver rules based on the EU HOS regulations and proposed an LNS-based on a column generation heuristic. Kok et al. (2011) developed a sequential insertion heuristic for the same problem. Rancourt et al. (2013) considered a rich VRP with multiple time windows, a heterogeneous fleet of vehicles, and the US HOS regulations. The authors presented several heuristic scheduling approaches within a unified tabu search algorithm and studied the performance of their algorithm on several benchmark sets. Goel and Irnich (2016) proposed the first exact algorithm for the VRTDSP, a branch-and-price algorithm considering the EU and the US HOS regulations. Their algorithm applies a DP labeling-based approach to create routes with schedules that comply to the given HOS regulations. Goel and Vidal (2014) introduced a hybrid genetic search for the VRTDSP and evaluated the impact of different HOS regulations on operating costs and accident risks, considering different HOS regulations. Koç et al. (2017) studied the VRTDSP with idling options using a comprehensive cost objective that takes idling costs into consideration.

1.4 Aims and organization of the paper

Our literature review reveals that no paper has yet proposed an integrated approach for mid and long-haul logistics capable of considering specific characteristics of ECVs (e.g., limited range and recharging times) as well as interdependencies between working shifts, time windows, and HOS regulations. Against this background, the aim of our paper is to present a detailed and generic analysis in order to compare competitiveness of ECVs against ICEVs and investigate the impact of HOS regulations on route patterns and costs. Herein, we first compare network operation of ECVs against ICEVs for a state of the art mid-haul logistics network without HOS regulation. Afterwards, we aim to analyze the impact of different HOS regulation schemes on the competitiveness of ECVs. Because recharging time can be accounted as break time (cf. European Union, 2006), we exploit the synchronization potential between idling times associated with battery recharging and driver break periods.

In order to achieve these aims, our methodology must be able to account for *i*) specific characteristics of the logistics network (distances, customer time windows, charging infrastructure), *ii*) the vehicle characteristics (driving range, recharging times), and *iii*) the HOS regulations (times until breaks, length of breaks, potential split breaks). This paper is the first to present a planning approach that integrates these requirements. Besides a mixed integer problem formulation for the respective planning tasks, we propose an ALNS metaheuristic capable of solving large-size, real-world instances. We use a two-step approach to derive insights for fleet operators and regulation authorities for *i*) the competitiveness of ECVs against ICEVs in general and *ii*) the impact of HOS regulations on this assessment and the general routing decision. Thus, we first derive results comparing ECVs to ICEVs without considering HOS regulations for current state-of-the-art mid-haul logistics. Second, we repeat this analysis but consider EU and US HOS regulations. Herein, we focus explicitly on the synergy effects between idle times induced by HOS regulations and recharging operations, and we assess the impact of HOS regulations on the competitiveness of ECVs.

The remainder of this paper is structured as follows. We first introduce a mixed integer problem formulation for our planning tasks in Section 2. Section 3 provides the description of our ALNS metaheuristic, and Section 4 describes our computational study. Results are discussed for EU and US HOS regulations, and managerial insights on the competitiveness of ECVs are presented. Section 5 concludes the paper.

2 Routing problems with truck driver scheduling for ICEVs and ECVs

We now present several mixed integer programs (MIPs) for our problem. We derived the formulations stepwise to better define the different planning tasks involved. In order to show how the models for the

proposed variants can be converted into each other by adding or neglecting certain constraints, we first introduce a common formulation for the VRPTW. We then extend this formulation to the VRP with truck driver scheduling (VRPTDS) and finally, we add further constraints to derive the EVRP with truck driver scheduling (EVRPTDS). The notation is summarized in Table 1.

The MIPs are defined on a complete directed graph $G = (\mathcal{V}, \mathcal{A})$ with a set of vertices $\mathcal{V}$ and a set of arcs $\mathcal{A}$. The set $\mathcal{V}$ is defined as the union of the sets $\mathcal{C}$, $\mathcal{R}$ and $\mathcal{B}$ described in the following. The set $\mathcal{C}$ denotes the customer vertices. Recharging is allowed at dedicated recharging vertices representing the location of charging stations. To allow for multiple visits to charging stations, we use dummy vertices. Thus, $\mathcal{R}$ denotes the set of all recharging vertices including dummy vertices to allow for multiple visits (cf. Schneider et al., 2014; Schiffer and Walther, 2017a). The set $\mathcal{B}$ contains the vertices that can be used specifically to take breaks. In addition, breaks are also allowed at customer and recharging vertices. The depot is represented by two vertices: 0 for the start depot and $n+1$ for the end depot. To include the start depot in one of the above mentioned sets, we use the subscripts 0 (e.g., $\mathcal{C}_0 = \mathcal{C} \cup \{0\}$) and $n+1$ for the end depot respectively. As is common, we define the cut set $\delta(\mathcal{S}) = \{(i,j) \in \mathcal{A} : i \in \mathcal{S}, j \in \mathcal{S}\}$ as the set of arcs with both endpoints in $\mathcal{S}$, where $\mathcal{S} \subseteq \mathcal{V}_{0n+1}$. Furthermore, the cut sets $\delta^+(\mathcal{S}) = \{(i,j) \in \mathcal{A} : i \in \mathcal{S}, j \notin \mathcal{S}\}$ and $\delta^-(\mathcal{S}) = \{(i,j) \in \mathcal{A} : i \notin \mathcal{S}, j \in \mathcal{S}\}$ define the outgoing and ingoing arcs of $\mathcal{S}$ respectively. If $\mathcal{S} = \{i\}$, we write $\delta(i)$ instead of $\delta(\{i\})$.

A time window defined by the interval $[e_i, l_i]$ is associated with each vertex. For the customer vertices $i \in \mathcal{C}$, e_i and l_i represent the earliest and latest start time of service, whereas for $i \in \mathcal{R} \cup \mathcal{B} \cup \{0, n+1\}$ the start and end of the scheduling horizon are given by e_i and l_i. In addition, each customer vertex has a demand p_i and a service time s_i ($p_i = s_i = 0, \forall i \notin \mathcal{C}$). The travel time t_{ij} from vertex i to vertex j is proportional to the distance d_{ij} because we assume a constant average vehicle speed v ($t_{ij} = v^{-1} d_{ij}$). A homogeneous fleet of vehicles with a freight capacity F is based at the depot. Fuel consumption and range limitations are neglected for ICEVs because of their large driving range and the ubiquitous availability of gas stations. For ECVs, the battery capacity Q is explicitly considered. We assume that energy consumption depends linearly on the traveled distance (with a consumption rate c). Analogously, the recharging time at a recharging vertex depends linearly on the amount of energy recharged (with a recharging rate r). These simplifications can be replaced by real-world data for the consumption on each arc or by more complex energy consumption functions (cf. Goeke and Schneider, 2015). In our objective we consider fixed route costs c^{fix} and distance-related operational costs c_{ij}.

To assess the influence of HOS regulations, breaks are modeled as follows. Drivers can take breaks at customer vertices, at recharging vertices, or at dedicated break vertices. Taking a break and recharging can occur simultaneously. However, breaks and customer service must be handled sequentially. Because we limit our investigations to single work shifts on a daily basis, we do not consider the rest periods of drivers. Thus, we limit the maximum tour duration to the time span until a longer rest has to take place (cf. Section 1.1). We use a generic modeling approach that can be applied to any HOS regulation as long as breaks can only be split into two partial breaks. Thus, we can investigate EU as well as US HOS regulations. Recall from Section 1.1, that the HOS regulations are based on three different durations that must not be exceeded: *i*) a full break has to be taken after C time units, *ii*) the overall driving time must not exceed D time units, and *iii*) the overall tour duration must not exceed E time units.

We provide a two-index formulation for each model, assigning vehicles to routes during post processing via backtracing. Thus, we use the binary variable x_{ij} to define whether arc (i,j) is traversed by a vehicle or not. To keep track of breaks, we denote by y_i the cumulative breaking time of the vehicle arriving at vertex i, counting breaks starting after the end of the last full break. In addition, z_i defines the time of a break at vertex i. The cumulated driving time after the last break up to vertex i is given by u_i, and the total driving time by g_i. The overall duration of a route up to vertex i includes service, recharging and slack times and is given by o_i. In order to calculate o_i, we additionally store the latest possible departure time at the depot to realize a minimum total duration m_i up to vertex i. The binary variable v_i indicates whether a break is completed at vertex i or not. The real variable τ_i represents the arrival time at vertex i, and the freight load of a vehicle at vertex i is given by f_i. If ECVs are considered, the real variable w_i denotes the amount of energy recharged at vertex i, and the battery load at vertex i is given by q_i.

Table 1: Sets, parameters, and decision variables.

Sets	
$0, n+1$	copies of the depot
$\mathcal{C}$	set of customer vertices
$\mathcal{R}$	set of potential recharging vertices including dummy vertices
$\mathcal{B}$	set of break locations
$\mathcal{V}$	set of all vertices without depot vertices ($\mathcal{C} \cup R \cup S$)
$\mathcal{A}$	set of arcs
Parameters	
c^{fix}	fixed route costs
c_{ij}	operational costs for arc (i,j)
e_i	earliest start time of service (recharge) allowed at vertex i
l_i	latest start time of service (recharge) allowed at vertex i
s_i	service time at vertex i
p_i	demand at vertex i
t_{ij}	travel time from vertex i to vertex j
d_{ij}	distance between vertex i and vertex j
r	recharging rate
c	consumption rate
b^{s}	time of a short break interval
b^{l}	time of a long (completed) break interval
Q	battery capacity
F	freight capacity
C	time after which a break has to be taken
D	maximum driving time
E	maximum total route duration
Decision variables	
x_{ij}	binary variable indicating whether arc (i,j) is traversed by a vehicle
y_i	cumulated break time after the last break at vertex i
z_i	break time at vertex i
u_i	cumulated driving time after the last break at vertex i
v_i	binary: break is completed at vertex i ($v_i = 1$) or not ($v_i = 0$)
g_i	total driving time up to vertex i
o_i	total duration up to vertex i
m_i	latest departure time at the depot to realize o_i
τ_i	start time of service (recharge, break) at vertex i
w_i	amount of energy charged at vertex i
q_i	battery load at vertex i
f_i	freight load at vertex i

The VRP variants considered in this paper are modeled as follows by means of directed two-index formulations:

VRPTW: A general VRPTW model is defined by (1)–(8).

minimize

$$Z = \sum_{(i,j)\in\delta^+(0)} c^{\text{fix}} x_{ij} + \sum_{(i,j)\in\mathcal{A}} c_{ij} x_{ij} \tag{1}$$

subject to

$$\sum_{(i,j)\in\delta^+(i)} x_{ij} = 1 \qquad i \in \mathcal{C} \tag{2}$$

$$\sum_{(i,j)\in\delta^-(j)} x_{ij} = \sum_{(i,j)\in\delta^+(j)} x_{ji} \qquad j \in \mathcal{V} \tag{3}$$

$$\tau_j \geq \tau_i + (t_{ij} + s_i)\, x_{ij} - l_0\,(1 - x_{ij}) \qquad i \in \mathcal{C}_0,\ (i,j) \in \delta^+(i) \tag{4}$$
$$e_i \leq \tau_i \leq l_i \qquad i \in \mathcal{V}_{0,n+1} \tag{5}$$
$$0 \leq f_j \leq f_i - p_i x_{ij} + F\,(1 - x_{ij}) \qquad (i,j) \in \mathcal{A} \tag{6}$$
$$0 \leq f_0 \leq F \tag{7}$$
$$x_{ij} \in \{0,1\} \qquad i \in \mathcal{V}_0,\ (i,j) \in \delta^+(i) \tag{8}$$

The objective minimizes overall costs, consisting of fixed costs for each tour c^{fix} and operational costs c_{ij} for driving (1). Constraints (2) ensure that each customer is visited exactly once, and constraints (3) ensure flow conservation. Constraints (4) relate the start time of service at consecutive vertices for customer locations, and constraints (5) guarantee time window feasibility for any vertex. Capacity constraints are defined by (6) and (7). Constraints (6) state that the amount of freight at vertex j is reduced by p_i if arc (i,j) is traveled, and constraint (7) limits the loading capacity of vehicles to F. Binary variables x_{ij} are defined in (8).

VRPTDS: Several extensions are necessary to integrate HOS regulations in the above formulation. Here we focus on the EU and US HOS regulations (see Section 1.1). In order to model them in a generic way, we define the cumulative breaking time y_i and the breaking time z_i at a vertex as discrete variables to allow full (long) and split (short, medium) breaks. Through constraints (9)–(13) the variables y_i and z_i are defined depending on the amount of time for a short break b^{s} and a long break b^{l}. This is done by using additional binaries y_i^k and z_i^k ($k \in \{\text{s},\text{m},\text{l}\}$), depending on whether a short (s), a medium (m) ($b^{\text{l}} - b^{\text{s}}$) or a long break (l) takes place at vertex i.

$$y_i = b^{\text{s}} y_i^{\text{s}} + b^{\text{l}} y_i^{\text{l}} \qquad i \in \mathcal{V}_{0,n+1} \tag{9}$$
$$b^{\text{s}} y_i^{\text{s}} + b^{\text{l}} y_i^{\text{l}} \leq 1 \qquad i \in \mathcal{V}_{0,n+1} \tag{10}$$
$$z_i = b^{\text{s}} z_i^{\text{s}} + \left(b^{\text{l}} - b^{\text{s}}\right) z_i^{\text{m}} + b^{\text{l}} z_i^{\text{l}} \qquad i \in \mathcal{V}_{0,n+1} \tag{11}$$
$$z_i^{\text{s}} + z_i^{\text{m}} + z_i^{\text{l}} \leq 1 \qquad i \in \mathcal{V}_{0,n+1} \tag{12}$$
$$y_i^{\text{s}},\ y_i^{\text{l}},\ z_i^{\text{s}},\ z_i^{\text{m}},\ z_i^{\text{l}} \in \{0,1\} \qquad i \in \mathcal{V}_{0,n+1}. \tag{13}$$

The VRPTDS can now be defined:

$$\sum_{(i,j) \in \delta^+(i)} x_{ij} \leq 1 \qquad i \in \{\mathcal{V} \setminus \mathcal{C}\} \tag{14}$$
$$\tau_j \geq \tau_i + (t_{ij} + s_i)\, x_{ij} + z_i - (l_0 + b^{\text{l}})\,(1 - x_{ij}) \qquad i \in \mathcal{V}_0,\ (i,j) \in \delta^+(i) \tag{15}$$
$$y_j \leq y_i + z_i + b^{\text{l}}\,(1 - x_{ij}) \qquad (i,j) \in \mathcal{A} \tag{16}$$
$$y_j \geq y_i + z_i - b^{\text{l}}\,(1 - x_{ij}) - b^{\text{l}} v_j \qquad (i,j) \in \mathcal{A} \tag{17}$$
$$y_j \leq z_i + b^{\text{l}}\,(1 - x_{ij}) + b^{\text{l}}\,(1 - v_j) \qquad (i,j) \in \mathcal{A} \tag{18}$$
$$C \geq u_j \geq u_i + t_{ij} x_{ij} - l_0\,(1 - x_{ij}) - l_0 v_i \qquad \forall (i,j) \in \delta(\mathcal{V}_0) \tag{19}$$
$$u_j \geq u_i + t_{ij} x_{ij} - l_0\,(1 - x_{ij}) \qquad \forall (i,j) \in \delta(\mathcal{V}_0) \tag{20}$$
$$D \geq g_j \geq g_i + t_{ij} x_{ij} - l_0\,(1 - x_{ij}) \qquad \forall (i,j) \in \delta(\mathcal{V}_0) \tag{21}$$
$$C \geq u_i + t_{ij} x_{ij} - l_0\,(1 - x_{ij}) - l_0 v_i \qquad \forall (i,j) \in \delta^-(n+1) \tag{22}$$
$$D \geq g_i + t_{ij} x_{ij} - l_0\,(1 - x_{ij}) \qquad \forall (i,j) \in \delta^-(n+1) \tag{23}$$
$$y_i \geq b^{\text{l}} v_i \qquad i \in \mathcal{V} \tag{24}$$
$$E \geq o_j \geq o_i + (s_i + t_{ij})\, x_{ij} - l_0\,(1 - x_{ij}) \qquad (i,j) \in \{\delta(\mathcal{V}_{0,n+1} \setminus \mathcal{R}) \cup \delta^+(\mathcal{R})\} \tag{25}$$
$$E \geq o_j \geq o_i + (w_i + t_{ij})\, x_{ij} - (l_0 + rQ)\,(1 - x_{ij}) \qquad (i,j) \in \delta^-(\mathcal{R}) \tag{26}$$
$$o_j \geq e_j - e_0 - m_i - l_0\,(1 - x_{ij}) \qquad (i,j) \in \{\delta(\mathcal{V}_{0,n+1} \setminus \mathcal{R}) \cup \delta^+(\mathcal{R})\} \tag{27}$$
$$0 \leq m_j \leq \begin{array}{l} o_i + (s_i + t_{ij})\, x_{ij} \\ \quad - l_j + e_0 + l_0\,(1 - x_{ij}) \end{array} \qquad (i,j) \in \{\delta(\mathcal{V}_{0,n+1} \setminus \mathcal{R}) \cup \delta^+(\mathcal{R})\} \tag{28}$$
$$0 \leq m_j \leq o_i + (w_i + t_{ij})\, x_{ij} - l_j + e_0 + l_0\,(1 - x_{ij}) \qquad (i,j) \in \delta^-(\mathcal{R}) \tag{29}$$

$$m_j \leq m_i + l_0 (1 - x_{ij}) \qquad (i,j) \in \{\delta (\mathcal{V}_{0,n+1} \setminus \mathcal{R}) \cup \delta^+ (\mathcal{R})\} \quad (30)$$
$$y_0 \leq 0 \quad (31)$$
$$z_0 \leq 0 \quad (32)$$
$$v_i \in \{0,1\} \qquad i \in \mathcal{V}. \quad (33)$$

Constraints (14) relax the single assignment for all vertices that are not customer vertices and do not have to be visited. To ensure that breaks are prohibited while providing service, we replace constraints (4) with constraints (15). Note that $s_i = 0 \ \forall i \in \{\mathcal{V}_{0,n+1} \setminus \mathcal{C}\}$ holds. Constraints (16)–(18) determine the cumulative break time for consecutive vertices. Constraints (16) and (17) propagate the cumulative break y_i until the next full break. Constraints (18) reset y_i after a full break has taken place. In combination with the domains of $y_i \in \{0; b^{\mathrm{s}}; b^{\mathrm{l}}\}$ and $z_i \in \{0; b^{\mathrm{s}}; b^{\mathrm{l}} - b^{\mathrm{s}}; b^{\mathrm{l}}\}$ (cf. (9)–(13)), constraints (16) and (17) force split breaks to take place in the right order (i.e., the short part of the break before the long part). The cumulated driving time after the last completed break is propagated by (19). If a break is completed at i ($v_i = 1$), then (19) is relaxed and (20) resets the driving time for the next route segment. Furthermore, (19) limits the cumulated driving time after a break to its allowed maximum. Analogously, the overall driving time on a route is propagated by (21), but never reset. Again, it is limited to its allowed maximum. Since both the cumulated driving time and the total driving time cannot be defined uniquely for the end depot, Constraints (22) and (23) extend (19) and (21) to yield the driving time limits for the last route segments. Constraints (24) ensure that v_i can only be equal to one (and thus u_i and y_i are reset) if a full break is completed. The overall duration of a route is propagated by (25)–(27). Depending on which constraint is tight, driving and service (25) or recharging (26) times, or the latest departure at the depot (27) in relation to the next time window are considered. The latest departure time at the depot is propagated in (28)–(30). The latest departure is either decreased by driving and service (28) or recharging (29) times if it decreases while traversing an arc. Otherwise it is forwarded with its current value to keep the total duration as low as possible (30). Initial values for y_i and z_i are defined by (31) and (32). Binary variables v_i are defined in (33).

EVRPTDS: Constraints (34)–(37) must be added to the previous model to consider range limitations and recharging of ECVs.

$$\tau_j \geq \tau_i + t_{ij} x_{ij} + r \ w_i - (l_0 + rQ)(1 - x_{ij}) \qquad i \in \mathcal{R},\ (i,j) \in \delta^+ (i) \quad (34)$$
$$0 \leq q_j \leq q_i + w_i - c \ d_{ij} x_{ij} + Q (1 - x_{ij}) \qquad (i,j) \in \mathcal{A} \quad (35)$$
$$w_i \leq 0 \qquad i \in \{\mathcal{V} \setminus \mathcal{R}\} \quad (36)$$
$$0 \leq q_i + w_i \leq Q \qquad i \in \mathcal{V}_{0,n+1}. \quad (37)$$

Constraints (34) extend the time constraints by recharging times. If $i \in \mathcal{R}$ and $i \in \mathcal{B}$, the tighter constraint of (15) and (34) holds to allow for simultaneous breaking and recharging. Constraints (35) guarantee energy balance, constraints (36) limit recharging to recharging vertices, and constraints (37) forbid overcharging. The combination of (35)–(37) prevents vehicles from running out of energy.

3 Adaptive large neighborhood search metaheuristic

The MIP for the EVRPTDS described in Section 2 can only solve instances that are too small to allow a proper assessment of the influence of HOS regulations. In order to solve larger instances, we have modified the ALNS metaheuristic of Schiffer et al. (2017), which proved to be competitive on a large range of VRPs with intermediate stops, a problem class in which the EVRPTDS also belongs. To account for HOS regulations, we have incorporated additional components and mechanisms in this algorithm. Section 3.1 provides a summary of our ALNS algorithm and of the modifications made to integrate HOS regulations in the search phases. Section 3.2 describes the scheduling component used to evaluate the feasibility of a path in the presence of HOS regulations.

3.1 Overview of the ALNS algorithm

To keep the paper concise, we only provide a brief overview of our algorithm, but we describe in detail the major changes made with respect to the algorithm of Schiffer et al. (2017). All basic operators and search procedures are the same as those of Schiffer et al. (2017).

Figure 1 provides a pseudocode of our algorithm. The corresponding notation is defined in Table 2. The algorithm is based on an ALNS algorithm extended by an intensification phase. After creating an initial solution, a destroy and repair phase is applied to create a new candidate solution σ' at each iteration. First, a destroy operator is selected from set $\mathcal{D}$ according to adaptive operator weights π to remove customers from the current solution σ. Second, a repair operator is chosen analogously from set $\mathcal{O}$ and is used to create the candidate solution σ' by inserting the removed customers. After each destroy and repair iteration, a local search (LS) procedure is applied to improve σ'if the objective value $\lambda(\sigma')$ of the candidate solution does not exceed $(1+\delta)$ times the objective value $\lambda(\sigma^*)$ of the best known solution (cf. Dueck, 1993). In the LS phase, the moves that are infeasible with respect to the HOS regulations are forbidden. However, violations of freight capacity, battery capacity and time windows are allowed and penalized using a generalized objective function as discussed in the next paragraph. As proposed by Cordeau et al. (2001), we treat infeasible and feasible solutions separately. At each iteration ι, the candidate solution σ' becomes the current solution σ if it improves it. If σ' further improves the best known solution σ^*, a feasible candidate solution σ'_{f} is generated from σ'. If σ'_{f} improves the best known feasible solution σ^*_{f}, σ'_{f} is forwarded to σ^*_{f}. After η^{al} iterations, the adaptive penalty weights are adjusted by a scoring system that reflects the success of each operator in the preceding iterations. Analogously, the weights of the penalty terms of the generalized cost function are adjusted after η^{p} iterations. The algorithm stops after reaching a maximum number $\eta^{\max}$ of iterations or a maximum number $\eta^{\max}_{\mathrm{noi}}$ of iterations without improvement.

```
1: σ ← initialSolution(), initializeParameters(), ι ← 0
2: while (ι < η^max) and (ι − ι_imp < η^max_noi) do
3:     σ' ← destroyAndRepair(D, O, π, σ)
4:     if (λ(σ') < λ(σ*)(1 + δ)) then
5:         σ' ← localSearch(σ)
6:     if (λ(σ') < λ(σ)) then
7:         σ ← σ'
8:         if (λ(σ') < λ(σ*)) then
9:             σ* ← σ'
10:        if (λ(σ') < λ(σ*_f)) then
11:            σ'_f ← generateFeasibleSolution(σ')
12:            if feasible(σ'_f) and (λ(σ'_f) < λ(σ*_f)) then
13:                σ*_f ← σ'_f
14:                ι_imp ← ι
15:    updateScores(σ'), updatePenalties(σ')
16:    ι ← ι + 1
```

Figure 1: Pseudocode of our ALNS algorithm.

Schiffer et al. (2017) based their algorithm on a generalized objective function that contains penalty terms for the violation of freight capacity, time windows and battery capacity. In order to extend this approach to violations of HOS regulations, we would have to include a penalty term for driver breaks. To this end, it is necessary to generate an optimal but not necessarily feasible break schedule minimizing the overall break violation on infeasible paths. The determination of such a schedule would require (at least) a dynamic programming component (cf. e.g., Goel and Irnich, 2016). However, the resulting computational complexity of such a procedure prevents the application within every search move. Therefore, the procedure of Schiffer et al. (2017) cannot be extended for driver breaks without losing a computational complexity of $O(1)$ for the evaluation of search moves. Thus, we work with the original generalized cost function of Schiffer et al. (2017),

Table 2: Parameters used in the ALNS algorithm.

$\mathcal{O}$ / $\mathcal{D}$	set of repair / destroy operators
$\mathcal{T}$	request bank to store temporally break-infeasible vertices
π	operator weights, reflecting the operators performance
σ' (σ'_{f}) /σ / σ^* (σ^*_{f})	candidate / current / best (feasible) solution
$\eta^{\max}$	maximum number of iterations
$\eta^{\max}_{\mathrm{noi}}$	maximum number of iterations without improvement
η^{al}	number of iterations after which the operator probabilities are adapted
η^{p}	number of iterations after which the penalty weights are adapted
δ	percentage deviation in which the local search is applied
ι	iteration count
ι_{imp}	iteration in which the last improvement was achieved
η^{req}	number of iterations after which the search mode is switched

calculating violations as described in Appendix A, and handle break violations separately as described in the following.

If the algorithm is used in this fashion, it may not lead to a break-feasible best solution. During the algorithm development, we found that there exists a trade-off between finding a good (break-feasible) solution and obtaining break feasibility at every iteration. Therefore we did not integrate additional operators to enforce break feasibility or limit all search moves to break-feasible moves. In order to account for both *i*) search phases in which the algorithm focuses on obtaining and improving break feasibility, and *ii*) search phases in which the algorithm accepts improving but break-infeasible solutions, our algorithm works in a two-phase mode, which switches every η^{req} iterations. In the `forceImprovement` mode, search moves are not restricted to break-feasible moves and every improvement is considered to overcome local optima. After η^{req} iterations in `forceImprovement` mode, the algorithm switches to the `forceBreakFeasibility` mode. In this mode, only search moves that yield a break-feasible route are allowed. To check break feasibility, the method described in Section 3.2 is used. After a destroy operator in `forceBreakFeasibility` mode has been applied, it may happen that single customers cannot be reinserted into the solution in a break-feasible manner and thus, incomplete solutions result. In this case, customers that cannot be reinserted in a repair step due to violated HOS regulations are placed in a request bank $\mathcal{T}$ which works in a first-in-first-out mode. Thus, nodes that were put in the request bank in the last destroy and repair iteration are first inserted into σ' at the next repair step. In both modes, solutions $(\sigma', \sigma^*, \sigma)$ are only forwarded to their feasible equivalent if they are break-feasible.

3.2 HOS evaluation

To conduct an HOS feasibility check on an arbitrary path ρ, we first generalize some characteristics of the HOS regulations and we derive properties of ρ that are used to efficiently determine whether a feasible breaking schedule exists. Although the EU and US HOS regulations differ with respect to time spans and split breaks, both contain a maximum allowed overall duration $T^{\max}$ before a driver has to take a rest. For a one-day planning horizon, $T^{\max}$ represents the maximum allowed duration of a path, including idle times due to breaks, recharging and providing service. Furthermore, the path is limited to a maximum driving time duration T^{drive} and a maximum driving time T^{break} after which a break must be taken. For these durations, (38) holds independent by the considered HOS regulations:

$$\frac{T^{\mathrm{drive}}}{2} \leq T^{\mathrm{break}} \leq T^{\mathrm{drive}} \leq T^{\max}. \tag{38}$$

To discuss the characteristics of an arbitrary path that are applicable to both HOS regulations, we define three additional sequences $T^{fwd} = T^{bwd} = T^{int} = T^{\mathrm{break}}$ which are all equal to the maximum duration that can be driven without a break, but differ with respect to their position on a path. These segments are illustrated in Figure 2. The sequence T^{fwd} is scheduled at the beginning of a path, while T^{bwd} is scheduled at the end of a path analogously. The sequence T^{int} is placed symmetrically in the middle of a path ρ for which $T^{\rho} > T^{\mathrm{break}}$ is valid. Note at this point that for paths on which the overall driving time T^{ρ} is less than

T^{break}, a break check is not necessary. Based on these definitions and the additionally resulting segments (I) and (II) (cf. Figure 2) and considering that the driving time of a path T^ρ is always smaller than T^{drive} if it is feasible, we can state the following propositions on HOS feasibility checks:

Proposition 1 *If at least one potential full break can be taken within* $[T^\rho - T^{bwd}, T^{fwd}]$ *(i.e., one break in segment (I)) then at least one feasible break schedule for* ρ *exists.*

Proposition 2 *If no potential full break within* $[T^\rho - T^{bwd}, T^{fwd}]$ *exists, then a full break in* $[\frac{T^\rho - T^{fwd}}{2}, T^\rho - T^{bwd}]$ *and a full break in* $[T^\rho - T^{fwd}, T^\rho - \frac{T^\rho - T^{fwd}}{2}]$ *(i.e., two breaks in (II)) are sufficient to obtain a feasible break schedule.*

Proposition 3 *If neither Proposition 1 nor Proposition 2 holds, a feasible break schedule exists if a potential full break within* $[\frac{T^\rho - T^{fwd}}{2}, T^\rho - T^{bwd}]$ *and a potential full break within* $[T^\rho - \frac{T^\rho - T^{fwd}}{2}, T^\rho - \frac{T^\rho - T^{fwd}}{2} + \Delta^{fwd}]$*, or if a potential full break within* $[T^\rho - T^{fwd}, T^\rho - \frac{T^\rho - T^{fwd}}{2}]$ *and* $[T^\rho - T^{bwd} - \Delta^{bwd}, T^\rho - T^{bwd}]$ *exists. In this case,* Δ^{bwd} *denotes the time between the end of the potential break in* $[T^\rho - T^{fwd}, T^\rho - \frac{T^\rho - T^{fwd}}{2}]$ *and* $[T^\rho - \frac{T^\rho - T^{fwd}}{2}]$*, while* Δ^{fwd} *denotes the time between the start of the potential full break in* $[\frac{T^\rho - T^{fwd}}{2}, T^\rho - T^{bwd}]$ *and* $[\frac{T^\rho - T^{fwd}}{2}]$*.*

Proposition 4 *If no potential full break can be realized in the interval* $[\frac{T^\rho - T^{fwd}}{2}, T^\rho - \frac{T^\rho - T^{fwd}}{2}]$*, then no feasible break schedule can be derived.*

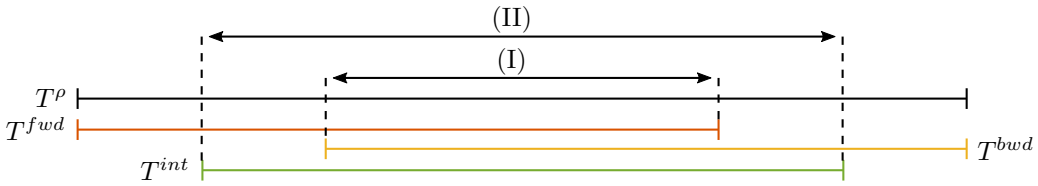

Figure 2: Possible segments in which a break has to be conducted in path ρ.

Note that these propositions hold without loss of generality since we immediately discard paths for which $T^\rho > T^{\text{drive}}$. Using the information of the penalty terms stated in Appendix A, we can compute the duration of an arbitrary segment. This information is used to identify violations in $T^{\max}$. Potential break times that can be taken before an arc (i, j) on a path is traversed or before service at j is provided, can be calculated by $l_j - a_j^{\min}$. Storing this information in a look-up table and bookkeeping the driving times for each path, HOS feasibility can be checked in constant time based on the above propositions.

4 Computational study

This section presents the results of our computational study to assess the impact of HOS regulations on the competitiveness of ECVs compared to ICEVs. We first describe the experimental setup and derive benchmark instances in Section 4.1. We then discuss the impact of HOS regulations focusing on the competitiveness of ECVs compared to ICEVs in Section 4.2.

All computational experiments were conducted on a standard desktop computer with an Intel Core i7 3.60 GHz processor and 16 GB RAM running Ubuntu 16.04 LTS. We implemented our algorithm as a single core thread in C++, using the parameter setting described in Schiffer et al. (2017) for all experiments. Only η^{req} was fitted according to the method described in Pisinger and Ropke (2007) and set to $\eta^{\text{req}} = 400$.

4.1 Experimental setup

In order to evaluate the competitiveness of ICEVs and ECVs as well as the impact of HOS regulations, we apply a two-step approach.

1. We first model the current state-of-the-art operation of mid-haul logistics using ICEVs. We then extend this model to handle ECVs regarding their specific characteristics (i.e., limited driving range, recharging processes). For both experiments, we first assume that the HOS regulations do not apply.
2. We then repeat the same analyses by now integrating the EU and the US HOS regulations. This allows us to analyze how a synchronization of idle times due to recharging and breaks can increase the competitiveness of ECVs compared with that of ICEVs in mid-haul transportation.

Comparing these results, we are able to derive insights on the competitiveness of ECVs compared to ICEVs. The results allow for an evaluation of the competitiveness of ECVs based on the state-of-the-art of current technological and network design restrictions. Furthermore, the influence of (different) HOS regulations can be extracted. All results are compared based on overall costs.

In order to perform the analyses, we created data sets that represent logistics networks with diverse structures. To avoid creating a bias due to structural limitations, instances must be based on real-world data, but must not be limited to single application cases respectively specific network structures. However, instances for ECV logistics fleets have so far been either artificially created (cf. Schneider et al., 2014) or limited to selected real-world application cases (cf. Schiffer et al., 2016). For instance, Schneider et al. (2014) designed artificial instances based on the well-known Solomon instances (cf. Solomon, 1987) by considering clustered, random and randomly-clustered customer distributions, but without applying a real-world distance metric or realistic recharging and consumption rates. Schiffer et al. (2016) derived real-world instances from an extensive field test of 12-tonne medium-duty ECVs in the logistics network of a German retail company. However, these instances are limited to a nearly uniform customer distribution.

To derive instances that consider real-world data on recharging times and energy consumption as well as varying customer patterns, we use the real-world data of a retailer network as described in Schiffer et al. (2016), but we adapt this case to the instances of Schneider et al. (2014) as follows:

1. The customer located furthest from the depot is selected. The distance between this customer and the depot is then fixed to 150km in order to model mid-haul distribution areas. All other distances are scaled proportionally.
2. The planning horizon is set to 960 minutes, accounting for a delivery period from 6h00 to 22h00 obtaining a depot time window $[e_0, l_0] = [0, 960]$. The original time windows of the customers are scaled proportionally.
3. Maximum tour durations, driving times and breaks are defined as in Section 1.1.
4. The battery capacity is set to $Q = 160$kWh, the energy consumption is set to $c = 0.73\frac{\text{kWh}}{\text{min}}$ and an inverse recharging rate of $r = 1.36\frac{\text{min}}{\text{kWh}}$ is considered, based on the data of the field test provided in Schiffer et al. (2016).
5. We used fixed costs for an ECV tour $c^{fix,e} = 53.32€$ and fixed costs for an ICEV tour $c^{fix,i} = 26.27€$, considering daily vehicle investment costs from Schiffer et al. (2016). Operational costs are set to $c^e = 0.0508\frac{€}{\text{km}}$ for ECVs and to $c^i = 0.2233\frac{€}{\text{km}}$ for ICEVs as in Schiffer et al. (2016).
6. Additional break vertices were placed on the 20% longest arcs, randomly on each arc in an interval of 25% to 75% of its length.

The derived sets differ with respect to the spatial customer distribution which is either clustered (c), randomly distributed (r) or randomly clustered (rc). Furthermore, they differ with respect of the considered freight capacity in relation to the customer demand. Sets of type 100 have a small vehicle freight capacity in order to model larger deliveries, while sets of type 200 show a large vehicle freight capacity to account for more fragmented deliveries. To quantify this difference, one can compare the vehicles' freight capacity divided by the average customer demand, which is between $[11, 14]$ for instances of type 100 and between $[38, 69]$ for instances of type 200. This means, that on average a vehicle can cover between 38 and 69 customers on a route for type 200 instances and only between 11 and 14 for type 100 instances.

4.2 Results

We now discuss the results of our study. We first briefly discuss the computational performance of our algorithm (Section 4.2.1). We then focus on the impact of HOS regulations, especially on the synchronization potential between recharging and breaking stops (Section 4.2.2). Finally, we evaluate the competitiveness of ECV against ICEV and discuss whether HOS regulations have a significant impact on the competitiveness evaluation of ECVs (Section 4.2.3). Detailed computational results are provided in Appendix B.

4.2.1 Computational performance

The box-whisker plot in Figure 3 shows the distribution of the average runtime out of ten runs t^a over all instances for the different problem variants. For ICEVs, we focus on the vehicle routing problem without HOS regulations (VRP), with US HOS regulations (VRP-US), and with EU HOS regulations (VRP-EU). Concurrently, we consider the electric vehicle routing problem without HOS regulations (EVRP), with US HOS regulations (EVRP-US), and with EU HOS regulations (EVRP-EU).

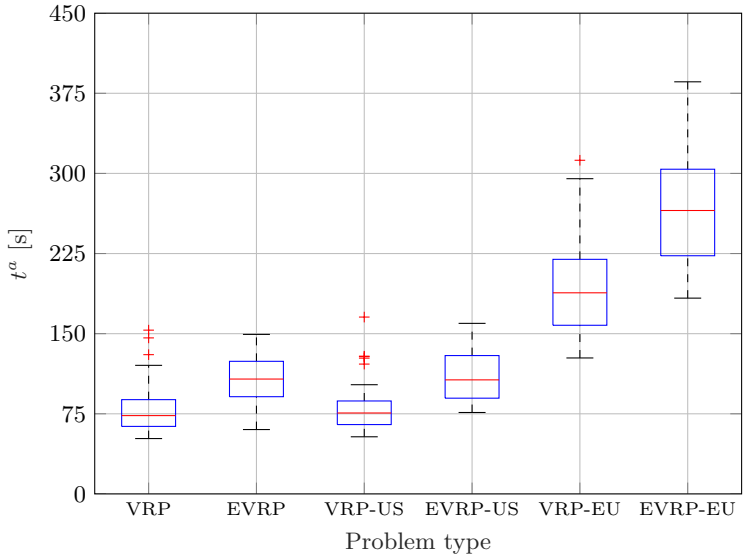

Figure 3: Average computational times for all problem variants and instances.

As can be seen, all EVRPs exhibit higher computational times than their VRP counterparts. Furthermore, for both the VRPs and the EVRPs, the instances with EU HOS regulations are the computationally most demanding. However, our algorithm provides relatively short runtime even for the EU HOS regulations, yielding an average runtime below 400 seconds even for the worst instance, and an average t^a of 266.5 seconds over all instances.

4.2.2 Impact of HOS regulations

Figures 4–7 show the driving times and the tour durations that result when solving the different instance sets without considering HOS regulations. For the VRP (Figures 4–5), driving times do not exceed the maximum driving time $T_{\text{US}}^{\text{drive}}, T_{\text{EU}}^{\text{drive}}$ allowed due to HOS regulations for type 100 instances. Also, all tour durations do not exceed the maximum duration $T_{\text{US}}^{\text{max}}, T_{\text{EU}}^{\text{max}}$. Most of the driving times do not even exceed the threshold after which a break has to be taken $T_{\text{US}}^{\text{break}}, T_{\text{EU}}^{\text{break}}$. Thus, breaks can be scheduled on most tours without changing the tour itself. Type 200 instances, show higher driving times and total tour durations than type 100 instances for the VRP. For these, most of the driving times exceed $T_{\text{EU}}^{\text{break}}$. Some instances even exceed $T_{\text{US}}^{\text{break}}$ and $T_{\text{EU}}^{\text{drive}}$. Thus, significant changes on routes are necessary when applying HOS regulations. For the EVRP (Figures 6–7), similar characteristics and effects result. While driving times are in general lower than for the

VRP due to limited driving ranges, larger total durations result due to additional recharging times. Thus, a large number of routes in the type 200 instances and even single routes in the type 100 instances exceed the maximum allowed duration $T^{\max}_{\text{US}}, T^{\max}_{\text{EU}}$, which requires significant changes when applying HOS regulations.

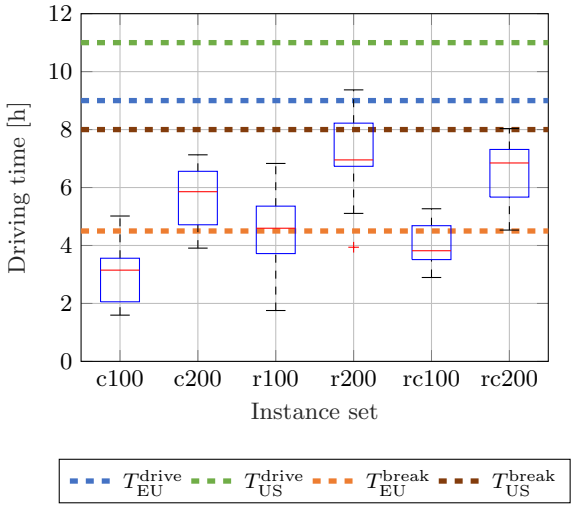

Figure 4: Driving times for the VRP.

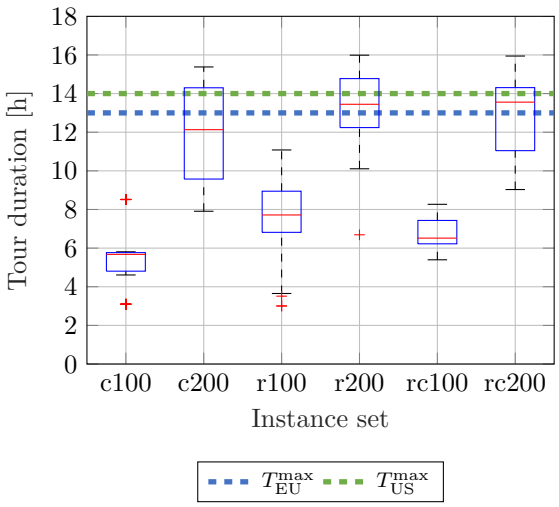

Figure 5: Tour durations for the VRP.

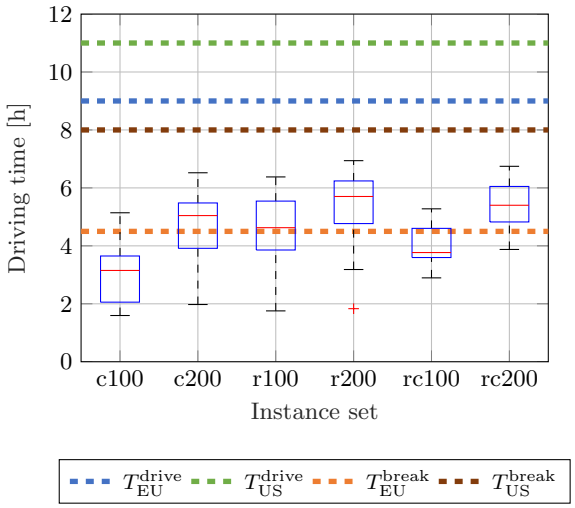

Figure 6: Driving times for the EVRP.

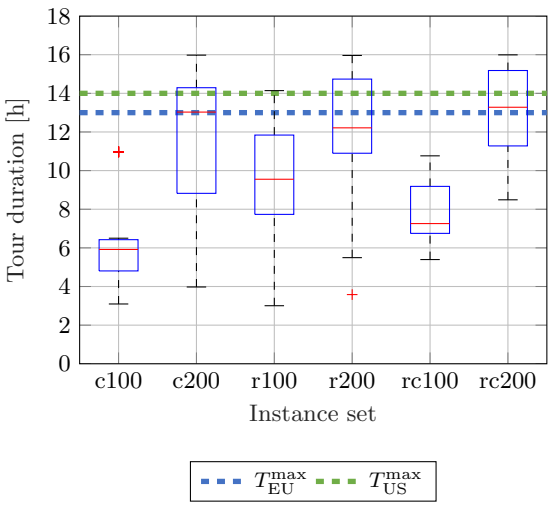

Figure 7: Tour durations for the EVRP.

To analyze the impact of applying HOS regulations, Table 3 shows the number of vehicles for the different instance sets and each problem variant. As can be seen, the number of vehicles remains equal for type 100 instance sets over all problem variants, while it increases for type 200 instance sets for both the VRP and the EVRP when applying HOS regulations. This shows, that for type 100 instances HOS can be scheduled on the given routes due to short driving times and tour durations, while routes have to be split and new solutions have to be created for type 200 instances.

To analyze how these increases in the number of vehicles and in routes affect the total costs, Table 4 shows the average percentage increase in total costs between the EVRP and the EVRP-US ($\Delta^{\text{ECV}}_{\text{US}}$), the EVRP and the EVRP-EU ($\Delta^{\text{ECV}}_{\text{EU}}$), and the EVRP-US and the EVRP-EU ($\Delta^{\text{ECV}}_{\text{US,EU}}$). Analogously, the mean percentage increase in total costs for the VRP approaches is stated. As can be seen, the consideration of HOS regulations has nearly no impact for instances of type 100, independent by the spatial customer distribution. Contrary,

significant increases in total average costs result on type 200 instances. For both the EVRP and the VRP the increase is the highest, if EU HOS regulations are applied.

The different effects between type 100 and type 200 instances are due to the characteristics of the initial solutions for the EVRP and the VRP without HOS regulations. For type 200 instances, more changes in routes are necessary to yield break-feasible solutions due to larger driving times and longer routes for which breaks have to be scheduled. In addition, several routes even exceed the maximum allowed tour duration. Thus, additional vehicles are necessary to derive feasible solutions for some instances. Overall, these changes lead to a significant increase in total costs. This increase is even higher for the EU HOS regulations because these are more restricting with respect to the maximum allowed duration and driving time.

Table 3: Number of vehicles for each instance set and problem variant.

Instance set	EVRP	EVRP-US	EVRP-EU	VRP	VRP-US	VRP-EU
c100	90	90	90	90	90	90
c200	41	46	48	32	33	40
r100	96	96	96	96	96	96
r200	67	72	77	45	55	55
rc100	72	72	72	72	72	72
rc200	41	48	50	32	39	40

Table 4: Mean increase in total costs for each instance set and problem variant.

Instance set	$\Delta^{\text{ECV}}_{\text{US}}$ [%]	$\Delta^{\text{ECV}}_{\text{EU}}$ [%]	$\Delta^{\text{ECV}}_{\text{US,EU}}$ [%]	$\Delta^{\text{ICEV}}_{\text{US}}$ [%]	$\Delta^{\text{ICEV}}_{\text{EU}}$ [%]	$\Delta^{\text{ICEV}}_{\text{US,EU}}$ [%]
c100	0.00	0.00	0.00	0.00	0.00	0.00
c200	10.56	15.18	4.56	3.47	10.58	6.93
r100	0.03	0.03	0.01	0.01	0.03	0.02
r200	6.00	12.02	5.99	6.73	7.71	0.93
rc100	0.00	0.00	0.00	0.02	0.06	0.04
rc200	14.37	18.24	3.56	6.33	7.85	1.45

The percentage increases are as follows: $\Delta^{\text{ECV}}_{\text{US}}$ - EVRP vs. EVRP-US, $\Delta^{\text{ECV}}_{\text{EU}}$ - EVRP vs. EVRP-EU, $\Delta^{\text{ECV}}_{\text{US,EU}}$ - EVRP-US vs. EVRP-EU, $\Delta^{\text{ICEV}}_{\text{US}}$ - VRP vs. VRP-US, $\Delta^{\text{ICEV}}_{\text{EU}}$ - VRP vs. VRP-EU, $\Delta^{\text{ICEV}}_{\text{US,EU}}$ - VRP-US vs. VRP-EU.

Although the previous results reveal the impact of HOS regulations on the number of vehicles and total costs, they are not sufficient to quantify the synchronization potential between recharging stops and drivers' breaks. To derive deeper insights, we analyze the synchronization potential as well as the instance specific violations in the following. Doing so, we highlight the benefit of the respective synchronization potential.

Table 5 shows the share of routes with recharging stops RS for each instance set for the EVRP variants. For these routes, the proportion BRS for which breaking stops can completely be synchronized with recharging stops is given. All but the c100 instances show a large share of routes with recharging stops. On average, at least 80% of these stops can be used for simultaneous breaking stops for both US and EU HOS regulations. Furthermore, the synchronization potential between breaking and recharging for EU HOS regulations is at least equal to the synchronization potential of US HOS regulations on any instance set, although the duration of breaks is higher in the US than in the EU. This shows that allowing for split breaks helps synchronize recharging and breaking and may even compensate larger breaking times.

Table 6 shows for each instance set and both problem types (EVRP, VRP) the number of routes that are infeasible due to *i*) the maximum tour duration (N^{max}), *ii*) the maximum driving time (N^{drive}), and *iii*) the maximum driving time without a break (N^{break}), for both US and EU regulations. Furthermore, we provide the number of instances for each instance set (n), and the number of instances for which the increase in total costs is greater than 1% ($\hat{\Delta}$) between the US and EU regulations. The latter is needed for further discussions because the average cost increases in Table 4 do not reflect increases that are either much smaller ($< 1\%$)

Table 5: Number of routes with (synchronized) recharging stops.

	EVRP	EVRP-US		EVRP-EU	
Instance set	*RS*	*RS*	*BRS*	*RS*	*BRS*
c100	50.00%	50.00%	55.56%	50.00%	55.56%
c200	97.56%	89.13%	97.56%	91.67%	97.73%
r100	80.21%	81.25%	85.90%	81.25%	96.15%
r200	98.51%	100.00%	88.89%	96.10%	88.89%
rc100	88.89%	88.89%	70.31%	88.89%	78.13%
rc200	100.00%	100.00%	83.33%	100.00%	92.00%
Average	85.86%	84.88%	80.26%	84.65%	84.74%

The abbreviations are as follows: *RS* - share of routes with recharge stops , *BRS* - share of recharge stops synchronized with breaks

Table 6: Number and type of HOS violations for each instance set and vehicle type.

		EVRP							VRP						
Set	n	$\hat{\Delta}$	N_{US}^{max}	N_{US}^{drive}	N_{US}^{break}	N_{EU}^{max}	N_{EU}^{drive}	N_{EU}^{break}	$\hat{\Delta}$	N_{US}^{max}	N_{US}^{drive}	N_{US}^{break}	N_{EU}^{max}	N_{EU}^{drive}	N_{EU}^{break}
c100	9	0	0	0	0	3	0	9	0	0	0	0	0	0	9
c200	8	2	24	0	0	24	0	24	7	8	0	0	16	0	24
r100	12	0	31	0	0	37	0	58	0	0	0	0	0	0	59
r200	11	5	46	0	0	51	0	57	6	12	0	13	24	6	44
rc100	8	0	0	0	0	0	0	18	0	0	0	0	0	0	22
rc200	8	2	30	0	0	31	0	34	3	10	0	1	18	0	32
total	56	9	131	0	0	146	0	200	16	30	0	14	58	6	190

The abbreviations are as follows: n - number of instances, $\hat{\Delta}$ - number of instances with a cost increase $> 1\%$ between US and EU regulations, N_{US}^{max} - infeasible routes due to the maximum tour duration (US), N_{EU}^{max} - infeasible routes due to the maximum tour duration (EU), N_{US}^{drive} - infeasible routes due to the maximum driving time (US), N_{EU}^{drive} - infeasible routes due to the maximum driving time (EU), N_{US}^{break} - infeasible routes due to the maximum driving time without a break (US), N_{EU}^{break} - infeasible routes due to the maximum driving time without a break (EU).

or significantly higher than the stated average value for type 200 instances. As can be seen, the number of total violations is much higher for the EVRP. However, violations due to T_{US}^{break} only arise for the VRP since routes for the EVRP remain shorter due to limited driving ranges. Based on the findings of Tables 4–6, the impact of the synchronization potential between recharging and driver breaks can be summarized as follows for each instance set:

c100: For this instance set, the number of infeasible routes is quite low. Only nine routes remain infeasible due to violations of T_{EU}^{break} for both problem variants, and three more routes remain infeasible for the EVRP due to violations of T_{EU}^{max}. In all cases, the synchronization potential is sufficient to realize necessary breaks due to HOS. Thus, the number of vehicles remains constant across all problem variants and the total costs remain equal for the EVRP and the VRP.

c200: The number of infeasible routes due to violations in T_{EU}^{break} is equal for both the EVRP and the VRP. However, significantly more violations of T_{EU}^{max} and T_{US}^{max} result for the EVRP. For two instances, a large increase in total costs exists when applying EU instead of US regulations. In these cases, the synchronization potential is not sufficient to realize all breaks. Thus, the large cost increase results out of an increase in the number of needed vehicles. For the VRP a large increase in costs remains for seven instances, since no synchronization potential is available for ICEVs.

r100: For the VRP infeasible routes result only due to violations in T_{EU}^{break}, while significantly more violations result for the EVRP out of violations in T_{US}^{max} and T_{EU}^{max}. However, the number of vehicles remains constant over all problem types and the increases in total costs are nearly zero for the EVRP. Thus, the synchronization potential is sufficient to realize all breaks for this instance set.

r200: Infeasible routes for the EVRP are due to violations in $T_{\text{US}}^{\max}$, $T_{\text{EU}}^{\max}$, and $T_{\text{EU}}^{\text{break}}$. For the VRP fewer violations result but these are spread on violations in $T_{\text{US}}^{\text{break}}$ and $T_{\text{EU}}^{\text{drive}}$, since there are no limitations on the driving range that would prevent routes with longer distances and driving times. For the EVRP five instances with large increases in total costs between the solution with US and the solution with EU HOS regulations remain. Thus, the synchronization potential is not sufficient to realize all breaks independent by the applied HOS regulations.

rc100: For this instance set even less violations arise for the EVRP than for the VRP due to limited driving ranges. All violations are due to $T_{\text{EU}}^{\text{break}}$. Again, the synchronization potential is sufficient to realize all necessary breaks.

rc200: Again, the total number of violations is higher for the EVRP but limited to violations in $T_{\text{US}}^{\max}$, $T_{\text{EU}}^{\max}$, and $T_{\text{EU}}^{\text{break}}$, while an additional violation in $T_{\text{US}}^{\text{break}}$ arises for the VRP.

Concluding, a significant synchronization potential between recharging and driver breaks exists and can contribute significantly to schedule breaks for ECVs. This synchronization potential is significantly higher in type 200 instances than in type 100 instances (cf. Table 5). This is mainly due to the fact that in type 200 instances more routes exist on which a break is necessary, while for type 100 instances, shorter routes without breaks remain. Accordingly, the overall number of routes with recharging stops is lower in type 100 instances compared to type 200 instances. In most cases, the synchronization allows to create feasible and rather robust solutions independent by the applied HOS regulations. Only for nine out of 56 instances does a significant increase in total costs arise when moving from US to EU HOS regulations. In general, violations for the EVRP are limited to violations in the maximum route duration for both regulations and maximum driving times without breaks for EU regulations, while violations for the VRP also arise due to violations in $T_{\text{US}}^{\text{break}}$ and $T_{\text{EU}}^{\text{drive}}$. However, fewer violations result for the VRP than for the EVRP. Furthermore, it should be noted that the number of instances with cost increases above 1% when applying EU instead of US regulations is higher for the VRP, because no synchronization potential can be used.

4.2.3 Competitiveness of ECVs against ICEVs

To evaluate the competitiveness of ECVs against ICEVs, we focus on the overall costs for different instance sets. Table 7 shows the difference in costs between the solution of the EVRP to the solution of the VRP without HOS regulations (ΔEVRP). Furthermore, the cost differences between the VRP and the EVRP are shown for the US (ΔEVRP-US) and EU regulations (ΔEVRP-EU). As can be seen, using ECVs instead of ICEV results in average cost savings of 18.47% without considering HOS regulations. This supports the results presented in Schiffer et al. (2016) for a mid-haul logistics network. If HOS regulations are applied, the average cost savings remain slightly above 20% for both US and EU regulations. This shows, that the synchronization potential between recharging and breaking increases the competitiveness of ECVs compared to ICEVs. While each break results in a change in the route plans for ICEVs, a large majority of the breaks for ECVs can be synchronized with recharging times, which are already considered in the route plans (cf. Section 4.2.2). The nearly equal cost savings for US and EU HOS regulations further back the finding of Section 4.2.2 that the synchronization potential also helps to reduce the impact of differences in break durations.

Table 7: Cost differences between the VRP and EVRP variants.

Instance set	ΔEVRP	ΔEVRP-US	ΔEVRP-EU
c100	12.31	12.31	12.31
c200	12.61	15.43	17.71
r100	27.38	27.39	27.40
r200	18.31	23.44	19.86
rc100	23.39	23.41	23.43
rc200	16.80	21.74	20.11
Average	18.47	20.62	20.14

The abbreviations are as follows: ΔEVRP [%] - cost difference between VRP and EVRP, ΔEVRP-US [%] - cost difference between VRP-US and EVRP-US, ΔEVRP-EU [%] - cost difference between VRP-EU and EVRP-EU.

5 Conclusion and outlook

We have introduced the EVRPTDS in order to assess the influence of HOS regulations on the operation of ECVs in mid-haul logistics fleets, with a special focus on their competitiveness against ICEVs. We have developed an ALNS metaheuristic with a time-efficient break-feasibility check and a request bank-based insertion mechanism to obtain break-feasible solutions. We created results following a two-step approach, first modeling the current state of the art for ECVs and ICEVs in mid-haul logistics without considering HOS regulations. Then we integrated EU and US HOS regulations respectively and analyzed changes in both route patterns as well as total costs and thus, the impact of HOS regulations on the competitiveness of ECVs and ICEVs. These experiments were conducted on newly created instances that cover both structural network differences and real-world technological characteristics for ECVs. Our results show that the integration of HOS regulations in routing problems affects the solutions, and that there is a large synchronization potential between recharging times and driver breaks for ECVs. Furthermore, our results demonstrate that ECVs are competitive against ICEVs in mid-haul logistics and that the benefit of ECVs is even larger if HOS regulations are considered and the respective synchronization potential is realized. In our case average cost savings of 18% are reached for the presented application case without considering the HOS regulations. Taking HOS regulations into account, these savings can be increased to at least 20%.

Appendices

A Penalty functions

In this section, we derive a penalty based evaluation approach for the EVRPTDS capable of calculating violations due to freight constraints, time window constraints and energy constraints, as well as providing path information that can be used to evaluate HOS feasibility of a path. To derive the necessary functions, we define the following auxiliary values:

a_{ij}^{slt} denotes the total slack time at vertex j, if arc (i,j) is traversed and the vehicle departs at the depot at e_0 (39).

a_{ij}^{slu} denotes the waiting time at vertex j, if arc (i,j) is traversed and the vehicle departs at the depot as late as possible in order to realize a minimum tour duration on a path (40).

a_{ij}^{addt} denotes the additional recharging time that is needed at the preceding charging station if arc (i,j) is traversed and a^{slt} is used for recharging implicitly (41).

a_{ij}^{addu} analogously denotes the additional recharging time that is needed at the preceding charging station if arc (i,j) is traversed and only a^{slu} is used for recharging implicitly (42).

$$a_{ij}^{\mathrm{slt}} = \max\left\{0, e_j - \tilde{a}_i^{\min} - t_{ij}\right\}, \tag{39}$$

$$a_{ij}^{\mathrm{slu}} = \max\left\{0, e_j - e_0 + a_i^{\mathrm{help}} - a_i^{\mathrm{dur}} - t_{ij}\right\}, \tag{40}$$

$$a_{ij}^{\mathrm{addt}} = \begin{cases} \max\left\{0, \max\left\{0, a_i^{\mathrm{rtt}} - a_{ij}^{\mathrm{slt}}\right\} + h_{ij} - H\right\} & \text{if } i \in \mathcal{R} \\ \max\left\{0, \max\left\{0, a_i^{\mathrm{rtt}} - \min\left\{a_{ij}^{\mathrm{slt}}, \tilde{a}_i^{\max} - \tilde{a}_i^{\min}\right\}\right\} + h_{ij} - H\right\} & \text{else,} \end{cases} \tag{41}$$

$$a_{ij}^{\mathrm{addu}} = \begin{cases} \max\left\{0, \max\left\{0, a_i^{\mathrm{rtu}} - a_{ij}^{\mathrm{slu}}\right\} + h_{ij} - H\right\} & \text{if } i \in \mathcal{R} \\ \max\left\{0, \max\left\{0, a_i^{\mathrm{rtu}} - \min\left\{a_{ij}^{\mathrm{slu}}, \tilde{a}_i^{\max} - \tilde{a}_i^{\min} + a_i^{\mathrm{rtu}} - a_i^{\mathrm{rtt}}\right\}\right\} + h_{ij} - H\right\} & \text{else.} \end{cases} \tag{42}$$

Using these auxiliary values, we define the following resources:

$a_i^{\min}$ denotes the earliest departure time at vertex i after providing service, recharging as few energy as necessary to keep the vehicle operational up to vertex i. $a_i^{\min}$ is propagated along an arc (i,j) using (43).

$a_i^{\max}$ denotes the earliest departure time at vertex i after providing service, recharging as much energy as possible at preceding charging stations. $a_i^{\max}$ is propagated along an arc (i,j) using (44).

a_i^{rtt} is the maximum amount of energy that can be recharged at vertex i if $i \in \mathcal{R}$ holds and the total slack time is used for recharging implicitly. Equation (45) is used to propagate a_i^{rtu}.

a_i^{rtt} analogously represents the maximum amount of energy that can be recharged at vertex i if $i \in \mathcal{R}$ holds and only the unavoidable slack time is used for recharging implicitly. In this case, equation (46) is used to propagate a_i^{rtu}.

a_i^{dur} denotes the minimum tour duration up to vertex i and is propagated in (47).

a_i^{help} is used to define the shift between the departure time of a vehicle and e_0 in order to realize a_i^{dur}. Equation (48) is used to propagate a_i^{help} along an arc (i, j).

a_i^{load} is used to state the cumulated customer demand of a path up to vertex i, including the demand of vertex i (49).

$$a_j^{\min} = \max\left\{e_j, \tilde{a}_i^{\min} + t_{ij}\right\} + s_j + a_{ij}^{\text{addt}}, \tag{43}$$

$$a_j^{\max} = \begin{cases} \max\left\{e_j, \tilde{a}_i^{\min} + a_i^{\text{rtt}} + t_{ij}\right\} + s_j & \text{if } i \in \mathcal{R} \\ \max\left\{e_j, \tilde{a}_i^{\max} + t_{ij}\right\} + s_j & \text{else,} \end{cases} \tag{44}$$

$$a_j^{\text{rtt}} = \begin{cases} \min\left\{H, \max\left\{0, a_i^{\text{rtt}} - a_{ij}^{\text{slt}}\right\} + h_{ij}\right\} & \text{if } i \in \mathcal{R} \\ \min\left\{H, \max\left\{0, a_i^{\text{rtt}} - \min\left\{a_{ij}^{\text{slt}}, \tilde{a}_i^{\max} - \tilde{a}_i^{\min}\right\}\right\} + h_{ij}\right\} & \text{else,} \end{cases} \tag{45}$$

$$a_j^{\text{rtu}} = \begin{cases} \min\left\{H, \max\left\{0, a_i^{\text{rtu}} - a_{ij}^{\text{slu}}\right\} + h_{ij}\right\} & \text{if } i \in \mathcal{R} \\ \min\left\{H, \max\left\{0, a_i^{\text{rtu}} - \min\left\{a_{ij}^{\text{slu}}, \tilde{a}_i^{\max} - \tilde{a}_i^{\min} + a_i^{\text{rtu}} - a_i^{\text{rtt}}\right\}\right\} + h_{ij}\right\} & \text{else,} \end{cases} \tag{46}$$

$$a_j^{\text{dur}} = \max\left\{a_i^{\text{dur}} + t_{ij}, e_j - e_0 + a_i^{\text{help}}\right\} + s_j + a_{ij}^{\text{addu}}, \tag{47}$$

$$a_j^{\text{help}} = \max\left\{a_i^{\text{dur}} + t_{ij} - l_j + e_0, a_i^{\text{help}}\right\} + a_{ij}^{\text{addu}}, \tag{48}$$

$$a_j^{\text{load}} = \min\left\{F, a_i^{\text{load}}\right\} + p_j. \tag{49}$$

Time traveled values $\tilde{a}_i^{\min}$ and $\tilde{a}_i^{\max}$ (cf. Schiffer and Walther, 2017a) of $a_i^{\min}$ and $a_i^{\max}$ are defined by (50) and (51).

$$\tilde{a}_i^{\min} = \min\left\{a_i^{\min}, a_i^{\max}, l_i + s_i\right\}, \tag{50}$$

$$\tilde{a}_i^{\max} = \min\left\{l_i + s_i, \min\left\{a_i^{\min}, a_i^{\max}, l_i + s_i\right\} + \max\left\{a_i^{\max} - a_i^{\min}, 0\right\}\right\}. \tag{51}$$

Initializing these resources by equations (52)–(54), time window ($\overrightarrow{TW}$), energy ($\overrightarrow{FL}$) and freight ($\overrightarrow{FR}$) constraint violations for a route ρ_i can be calculated by (55)–(57).

$$a_0^{\text{load}} = a_0^{\text{rtt}} = a_0^{\text{rtu}} = a_0^{\text{F}} = a_0^{\text{dur}} = 0, \tag{52}$$

$$a_0^{\min} = a_0^{\max} = e_0, \tag{53}$$

$$a_0^{\text{help}} = -l_0 + e_0, \tag{54}$$

$$\overrightarrow{TW}(\rho_i) = \sum_{v \in \rho_i} \max\left\{\min\left\{a_v^{\min}, a_v^{\max}\right\} - l_v, 0\right\}, \tag{55}$$

$$\overrightarrow{FL}(\rho_i) = \sum_{v \in \rho_i} \max\left\{a_v^{\min} - a_v^{\max}, 0\right\}, \tag{56}$$

$$\overrightarrow{FR}(\rho_i) = \sum_{v \in \rho_i} \max\left\{0, a_v^{\text{load}} - F\right\}. \tag{57}$$

For extensive explanations on the corridor based penalty approach we refer to Schiffer and Walther (2017a).

Backward penalty terms b_i^{κ}, $\kappa \in \{\text{min, max, slt, slu, rtt, rtu, addt, addu, F, dur, help, load}\}$ to evaluate a path backward are derived from the forward terms by swapping e_i and l_i and multiplying time-dependent components by -1:

$$b_{ji}^{\text{slt}} = \max\left\{0, -l_i - s_i + \tilde{b}_j^{\min} - t_{ji}\right\}, \tag{58}$$

$$b_{ji}^{\text{slu}} = \max\left\{0, -l_i - s_i + l_{n+1} + b_j^{\text{help}} - b_j^{\text{dur}} - t_{ji}\right\}, \tag{59}$$

$$b_{ji}^{\text{addt}} = \begin{cases} \max\left\{0, \max\left\{0, b_j^{\text{rtt}} - b_{ji}^{\text{slt}}\right\} + h_{ji} - H\right\} & \text{if } j \in \mathcal{R} \\ \max\left\{0, \max\left\{0, b_j^{\text{rtt}} - \min\left\{b_{ji}^{\text{slt}}, \tilde{b}_j^{\min} - \tilde{b}_j^{\max}\right\}\right\} + h_{ji} - H\right\} & \text{else,} \end{cases} \tag{60}$$

$$b_{ji}^{\text{addu}} = \begin{cases} \max\left\{0, \max\left\{0, b_j^{\text{rtu}} - b_{ji}^{\text{slu}}\right\} + h_{ji} - H\right\} & \text{if } j \in \mathcal{R} \\ \max\left\{0, \max\left\{0, b_j^{\text{rtu}} - \min\left\{b_{ji}^{\text{slu}}, \tilde{b}_j^{\min} - \tilde{b}_j^{\max} + b_j^{\text{rtu}} - b_j^{\text{rtt}}\right\}\right\} + h_{ji} - H\right\} & \text{else,} \end{cases} \tag{61}$$

$$b_i^{\min} = \min\left\{l_i + s_i, \tilde{b}_j^{\min} - t_{ji}\right\} - s_i - b_{ji}^{\text{addt}}, \tag{62}$$

$$b_i^{\max} = \begin{cases} \min\left\{l_i + s_i, \tilde{b}_j^{\min} - b_j^{\text{rtt}} - t_{ji}\right\} - s_i & \text{if } j \in \mathcal{R} \\ \min\left\{l_i + s_i, \tilde{b}_j^{\max} - t_{ji}\right\} - s_i & \text{else,} \end{cases} \tag{63}$$

$$b_i^{\text{rtt}} = \begin{cases} \min\left\{H, \max\left\{0, b_j^{\text{rtt}} - b_{ji}^{\text{slt}}\right\} + h_{ji}\right\} & \text{if } j \in \mathcal{R} \\ \min\left\{H, \max\left\{0, b_j^{\text{rtt}} - \min\left\{b_{ji}^{\text{slt}}, \tilde{b}_j^{\min} - \tilde{b}_j^{\max}\right\}\right\} + h_{ji}\right\} & \text{else,} \end{cases} \tag{64}$$

$$b_i^{\text{rtu}} = \begin{cases} \min\left\{H, \max\left\{0, b_j^{\text{rtu}} - b_{ji}^{\text{slu}}\right\} + h_{ji}\right\} & \text{if } j \in \mathcal{R} \\ \min\left\{H, \max\left\{0, b_j^{\text{rtu}} - \min\left\{b_{ji}^{\text{slu}}, \tilde{b}_j^{\min} - \tilde{b}_j^{\max} + b_j^{\text{rtu}} - b_j^{\text{rtt}}\right\}\right\} + h_{ji}\right\} & \text{else,} \end{cases} \tag{65}$$

$$b_i^{\text{dur}} = \max\left\{b_j^{\text{dur}} + t_{ji}, -l_i - s_i + l_{n+1} + b_j^{\text{help}}\right\} + s_i + b_{ji}^{\text{addu}}, \tag{66}$$

$$b_i^{\text{help}} = \max\left\{b_j^{\text{dur}} + t_{ji} + e_i + s_i - l_{n+1}, b_j^{\text{help}}\right\} + b_{ji}^{\text{addu}}, \tag{67}$$

$$b_i^{\text{load}} = \min\left\{F, b_j^{\text{load}}\right\} + p_i, \tag{68}$$

$$\tilde{b}_i^{\min} = \max\left\{b_i^{\min}, b_i^{\max}, e_i + s_i\right\}, \tag{69}$$

$$\tilde{b}_i^{\max} = \max\left\{e_i + s_i, \max\left\{b_i^{\min}, b_i^{\max}, e_i + s_i\right\} - \max\left\{b_i^{\min} - b_i^{\max}, 0\right\}\right\}, \tag{70}$$

$$b_{n+1}^{\text{load}} = b_{n+1}^{\text{rtt}} = b_{n+1}^{\text{rtu}} = b_{n+1}^{\text{F}} = b_{n+1}^{\text{dur}} = 0, \tag{71}$$

$$b_{n+1}^{\min} = b_{n+1}^{\max} = l_{n+1}, \tag{72}$$

$$a_{n+1}^{\text{help}} = -l_{n+1} + e_{n+1}, \tag{73}$$

$$\overleftarrow{TW}(\rho_i) = \sum_{v \in \rho_i} \max\left\{e_v - \max\left\{b_v^{\max}, b_v^{\min}\right\}, 0\right\}, \tag{74}$$

$$\overleftarrow{FL}(\rho_i) = \sum_{v \in \rho_i} \max\left\{b_v^{\max} - b_v^{\min}, 0\right\}, \tag{75}$$

$$\overleftarrow{FR}(\rho_i) = \sum_{v \in \rho_i} \max\left\{0, b_v^{\text{load}} - F\right\}. \tag{76}$$

With these penalty terms, overall violations for freight constraints, time window constraints and energy constraints can be calculated in constant time if inserting a vertex $\langle v \rangle$ between two partial routes $\rho_1 = \langle 0, ..., x \rangle$ and $\rho_2 = \langle y, ..., n+1 \rangle$ to construct a route $\rho_e = \langle 0, ..., x, v, y, ..., n+1 \rangle$. While the calculation of freight violations is obvious, time window ($TW(\rho_e)$) and energy (FL) violations hold as derived in Schiffer and Walther (2017a) and stated in (77)–(78). These equations can also be simplified to the concatenation of two partial routes without inserting an additional vertex (cf. Schiffer and Walther, 2017a):

$$\begin{aligned} TW(\rho_e) = \overrightarrow{TW}(\rho_1) + \overleftarrow{TW}(\rho_2) + \max\left\{0, a_v^{\min} - l_v - s_v - \max\left\{0, a_v^{\min} - a_v^{\max}\right\}\right\} \\ + \max\left\{0, \min\left\{l_v + s_v, \max\left\{e_v, a_v^{\min}\right\}\right\} - b_v^{\min} - s_v - \max\left\{b_v^{\max} - b_v^{\min}, 0\right\}\right\} \end{aligned} \tag{77}$$

$$FL(\rho_e) = \overrightarrow{FL}(\rho_1) + \overleftarrow{FL}(\rho_2) + \max\left\{0, a_v^{\min} - a_v^{\max}\right\} + \max\left\{0, b_v^{\max} - b_v^{\min}\right\} + B, \tag{78a}$$

$$B = \begin{cases} \max\left\{0, a_v^{\text{rtt}} + b_v^{\text{rtt}} - H - \min\left\{a_v^{\text{rtt}}, \max\left\{0, b_v^{\min} - a_v^{\min} + s_v\right\}\right\}\right\} & \text{if } v \in \mathcal{R} \\ \max\left\{0, a_v^{\text{rtt}} + b_v^{\text{rtt}} - H - \min\left\{a_v^{\text{rtt}}, \min\left\{\max\left\{0, b_v^{\min} - a_v^{\min} + s_v\right\}, \right.\right.\right. & \text{else.} \\ \left.\left.\left. \max\left\{0, a_v^{\max} - a_v^{\min}\right\} + \max\left\{0, b_v^{\min} - b_v^{\max}\right\}\right\}\right\}\right\} \end{cases} \tag{78b}$$

B Detailed computational results

Table 8: Results for the VRP variants.

	VRPTW			VRPTDS-US			VRPTDS-EU		
Instance	λ^b	λ^a	t^a	λ^b	λ^a	t^a	λ^b	λ^a	t^a
c101	731.44	733.26	68.40	731.44	732.37	79.49	731.44	731.62	180.58
c102	730.76	732.12	88.40	730.76	732.01	72.46	730.76	731.13	196.86
c103	730.76	731.05	57.74	730.76	731.08	61.45	730.76	730.76	130.06
c104	730.76	731.33	51.82	730.76	731.15	68.08	730.76	730.76	128.40
c105	730.76	731.04	55.45	730.76	731.32	70.91	730.76	730.76	157.98
c106	730.76	731.12	65.53	730.76	731.10	56.33	730.76	730.76	127.27
c107	730.76	731.26	57.19	730.76	730.76	80.15	730.76	730.76	136.39
c108	730.76	731.03	66.83	730.76	731.08	54.59	730.76	730.76	133.88
c109	730.76	731.28	53.56	730.76	731.07	58.08	730.76	730.76	136.88
c201	457.47	457.77	57.81	469.70	499.43	59.48	505.97	506.52	156.90
c202	457.14	462.21	56.23	469.37	496.46	63.24	505.97	506.22	157.75
c203	457.14	459.28	64.41	469.37	498.60	69.13	505.97	506.25	239.28
c204	457.14	462.87	62.86	467.24	468.54	75.27	505.97	508.12	204.64
c205	457.14	476.37	66.48	469.37	490.80	90.64	505.97	507.59	182.74
c206	457.14	460.19	63.08	469.70	501.44	72.15	505.97	507.65	183.81
c207	460.27	494.05	80.39	504.05	505.18	58.67	505.97	506.41	187.93
c208	457.14	462.99	68.18	468.91	488.03	127.10	505.97	506.90	174.88
r101	763.57	767.71	90.19	764.41	768.70	121.53	764.41	767.63	236.74
r102	764.41	767.20	95.89	764.41	766.96	84.86	764.41	767.69	239.72
r103	764.41	768.36	78.24	764.41	767.66	87.03	764.41	766.86	200.41
r104	763.57	767.91	71.12	763.57	766.40	77.42	764.41	766.53	170.22
r105	763.57	767.73	88.09	763.57	768.29	66.91	763.57	765.42	216.01
r106	763.57	767.79	71.49	763.57	767.24	79.28	763.57	766.06	188.57
r107	763.57	767.28	90.98	763.57	767.28	80.89	764.99	766.66	191.25
r108	763.57	767.81	76.93	763.57	767.11	83.57	763.57	765.90	173.76
r109	764.41	767.33	73.47	764.41	766.82	80.33	764.41	765.86	242.27
r110	763.57	766.62	73.16	763.57	766.54	86.99	763.57	766.24	188.64
r111	763.57	766.82	85.21	763.57	766.87	82.08	763.57	765.70	201.50
r112	764.41	768.02	84.85	764.41	767.54	70.85	764.41	765.98	218.99
r201	621.45	644.82	130.36	624.22	654.34	128.93	633.71	663.65	285.17
r202	587.71	620.66	120.36	617.54	641.72	128.55	622.48	659.11	289.96
r203	576.58	615.82	146.05	617.95	626.28	165.54	619.09	648.63	295.06
r204	567.27	577.21	78.54	612.02	615.95	100.18	614.96	617.73	220.17
r205	565.96	587.85	91.60	608.75	613.00	72.61	614.96	615.75	161.37
r206	565.68	572.31	82.49	608.75	611.98	83.36	615.63	617.66	237.49
r207	565.68	572.54	87.20	609.84	613.08	84.01	615.63	617.68	230.96
r208	565.96	570.83	74.45	608.75	615.46	57.26	615.63	617.23	209.58
r209	566.23	570.29	101.95	609.84	616.29	102.22	615.63	624.39	228.11
r210	565.68	573.47	109.49	608.75	615.60	76.25	614.96	626.48	190.11
r211	565.96	568.72	78.16	608.75	614.37	69.57	614.96	617.89	243.60
rc101	795.14	797.74	65.40	795.14	798.56	60.29	795.14	798.93	173.03
rc102	795.14	797.69	72.37	795.14	798.60	66.74	795.14	797.47	172.10
rc103	795.14	798.42	57.82	795.14	797.63	68.95	797.53	798.22	141.56
rc104	795.14	798.81	59.36	795.14	798.69	64.73	795.14	798.08	139.33
rc105	794.96	798.56	61.88	794.96	798.21	62.34	794.96	797.37	165.56
rc106	794.96	798.66	69.49	794.96	798.68	65.09	794.96	797.62	147.93
rc107	794.96	797.48	63.35	796.31	799.66	72.05	796.31	797.61	183.50
rc108	794.96	798.23	58.52	794.96	797.40	53.48	794.96	796.32	206.30
rc201	536.39	547.13	153.30	554.38	565.33	88.79	555.21	594.07	194.75
rc202	516.36	536.03	94.71	549.80	551.29	93.86	551.59	553.90	312.31
rc203	508.52	527.22	79.57	545.32	550.33	89.00	551.65	554.22	225.60
rc204	510.42	526.19	80.57	545.32	547.86	99.75	551.82	553.59	157.61
rc205	510.28	528.03	61.67	545.32	548.90	61.06	550.30	550.57	136.96
rc206	504.56	510.86	97.23	518.96	546.04	100.04	550.30	551.57	168.98
rc207	502.65	507.39	99.06	545.32	546.76	76.90	550.30	551.20	144.47
rc208	502.65	503.36	66.71	545.32	545.70	55.72	550.30	551.04	215.38
Average			73.43			74.44			179.35

The abbreviations are as follows: λ^b - best objective function value out of ten runs, λ^a - average objective function value out of ten runs, t^a [s] - average computational time out of ten runs.

Table 9: Results for the EVRP variants.

	EVRPTW			EVRPTDS-US			EVRPTDS-EU		
Instance	λ^b	λ^a	t^a	λ^b	λ^a	t^a	λ^b	λ^a	t^a
c101	641.03	654.53	96.24	641.03	649.02	88.91	641.03	641.23	258.41
c102	640.88	642.13	78.30	640.88	641.04	104.55	640.88	640.89	198.54
c103	640.88	641.10	79.62	640.88	647.89	78.90	640.88	640.96	217.17
c104	640.88	640.98	104.39	640.88	653.46	76.22	640.88	640.89	187.92
c105	640.88	653.55	113.65	640.88	647.20	88.49	640.88	640.88	195.76
c106	640.88	654.10	68.48	640.88	648.61	81.92	640.88	640.89	197.16
c107	640.88	640.97	70.82	640.88	641.58	98.96	640.88	641.19	198.82
c108	640.88	654.12	60.25	640.88	641.07	77.64	640.88	640.88	194.98
c109	640.88	642.22	80.79	640.88	641.48	80.12	640.88	640.98	198.57
c201	355.09	396.00	100.63	414.21	433.20	149.71	416.59	433.82	287.58
c202	355.09	390.10	105.58	413.79	432.58	122.76	416.68	461.41	278.75
c203	354.83	407.03	93.22	413.63	426.89	89.20	416.68	439.40	213.91
c204	356.78	395.98	90.74	357.31	409.31	81.96	416.42	461.19	222.50
c205	354.83	372.78	107.82	415.53	455.56	85.72	415.53	428.48	347.21
c206	412.11	413.33	77.85	412.77	438.49	113.58	415.61	439.54	281.79
c207	355.39	401.53	104.62	356.90	431.81	150.02	416.59	450.48	227.69
c208	354.82	401.94	74.48	414.69	444.61	90.04	416.66	445.66	246.79
r101	554.82	568.05	119.13	554.82	567.71	153.95	555.25	567.58	355.25
r102	554.68	573.56	143.15	555.66	574.34	141.12	555.80	562.27	297.45
r103	554.77	568.06	118.23	555.04	568.09	142.48	555.04	561.60	311.00
r104	554.90	567.82	108.55	554.90	562.31	120.17	554.90	578.44	284.74
r105	554.51	556.26	136.59	554.51	573.66	128.21	554.51	561.50	315.90
r106	554.51	567.84	101.63	554.51	556.80	146.69	554.51	561.53	338.98
r107	554.51	561.50	112.58	555.00	568.36	102.37	555.00	567.39	276.13
r108	554.50	562.09	124.50	554.50	574.25	105.70	554.50	561.50	290.23
r109	554.51	556.10	124.11	554.51	561.95	107.82	554.51	561.33	256.08
r110	554.29	573.74	129.22	554.29	567.77	120.83	554.29	566.95	365.34
r111	554.51	573.42	143.47	554.51	556.12	133.14	554.51	561.34	320.78
r112	554.29	561.98	104.87	554.29	561.43	132.39	554.29	561.61	385.75
r201	439.38	503.09	127.09	495.71	531.95	136.64	497.85	549.09	267.63
r202	495.35	508.35	116.98	495.66	537.43	114.39	495.71	502.04	296.66
r203	438.77	485.26	146.32	495.17	525.99	110.65	495.17	507.72	331.43
r204	436.91	455.65	136.93	493.91	501.68	138.30	494.69	501.40	332.47
r205	437.20	455.22	140.04	437.26	483.92	136.03	494.65	507.08	269.51
r206	436.90	466.77	107.27	437.29	484.47	125.20	495.10	519.03	290.48
r207	436.60	438.13	145.93	439.13	484.48	123.11	495.18	507.65	311.25
r208	436.53	438.46	114.02	437.82	478.23	159.66	494.75	496.02	268.23
r209	437.03	443.53	141.65	494.01	496.56	108.92	494.65	513.18	326.58
r210	436.87	455.51	131.56	493.89	495.42	130.79	494.65	501.76	320.37
r211	437.14	443.76	149.32	437.96	483.36	152.78	494.65	501.54	305.83
rc101	608.83	609.96	103.97	608.83	609.72	88.80	608.83	609.66	233.50
rc102	609.36	621.23	76.81	609.36	609.97	93.11	609.36	609.64	251.53
rc103	609.36	609.89	86.52	609.36	615.37	82.16	609.36	609.48	251.58
rc104	609.27	615.53	92.64	609.27	615.34	108.74	609.36	615.44	204.14
rc105	609.36	609.96	88.43	609.36	615.65	98.54	609.36	609.54	262.95
rc106	608.83	615.23	82.11	608.83	615.59	101.27	608.83	609.55	223.39
rc107	608.76	620.67	91.28	608.76	615.98	90.64	608.76	609.63	221.31
rc108	608.93	609.77	91.93	608.93	609.74	88.64	608.93	609.48	258.24
rc201	424.68	450.16	89.71	427.12	479.54	113.20	484.05	502.67	218.09
rc202	366.20	413.31	107.78	426.23	461.74	104.08	483.96	484.54	248.70
rc203	365.50	394.92	120.18	425.76	449.62	96.28	428.17	478.93	183.27
rc204	365.17	382.97	123.62	425.09	431.86	87.96	425.40	455.23	273.24
rc205	365.53	377.76	114.75	425.04	431.42	99.20	426.04	455.49	234.66
rc206	365.70	419.08	102.67	424.63	425.73	98.47	425.40	449.37	302.02
rc207	364.88	378.46	118.82	424.60	425.33	100.06	425.55	461.09	243.19
rc208	365.17	377.62	124.15	424.71	425.25	124.33	425.96	444.07	245.51
Average			107.96			110.81			266.55

The abbreviations are as follows: λ^b - best objective function value out of ten runs, λ^a - average objective function value out of ten runs, t^a [s] - average computational time out of ten runs.

References

Archetti, C., M. W. P. Savelsbergh. 2009. The trip scheduling problem. Transportation Science 43(4) 417–431.

Bektaş, T., G. Laporte. 2011. The pollution-routing problem. Transportation Research Part B: Methodological 45(8) 1232–1250. Supply chain disruption and risk management.

Ceselli, A., G. Righini, M. Salani. 2009. A column generation algorithm for a rich vehicle-routing problem. Transportation Science 43(1) 56–69.

Conrad, R. G., M. A. Figliozzi. 2011. The recharging vehicle routing problem. T. Doolen, E. Van Aken, eds., Proceedings of the 2011 Industrial Engineering Research Conference. Reno, NV, 1–8.

Cordeau, J.-F., G. Laporte, A. Mercier. 2001. A unified tabu search heuristic for vehicle routing problems with time windows. Journal of the Operational Research Society 52(8) 928–936.

Davis, B. A., M. A. Figliozzi. 2013. A methodology to evaluate the competitiveness of electric delivery trucks. Transportation Research Part E: Logistics and Transportation Review 49(1) 8–23.

Desaulniers, G., F. Errico, S. Irnich, M. Schneider. 2016. Exact algorithms for electric vehicle-routing problems with time windows. Operations Research 64(6) 1388–1405.

Dueck, G. 1993. New optimization heuristics: The great deluge algorithm and the record-to-record travel. Journal of Computational physics 104(1) 86–92.

Erdoğan, S., E. Miller-Hooks. 2012. A green vehicle routing problem. Transportation Research Part E: Logistics and Transportation Review 48(1) 100–114.

European Union. 2006. Regulation (EC) no 561/2006 of the European parliament and of the council. http://eur-lex.europa.eu/legal-content/EN/TXT/?uri=CELEX%3A02006R0561-20150302 (last accessed: 07.06.17).

Felipe, Á., M. T. Ortuño, G. Righini, G. Tirado. 2014. A heuristic approach for the green vehicle routing problem with multiple technologies and partial recharges. Transportation Research Part E: Logistics and Transportation Review 71 111–128.

Feng, W., M. Figliozzi. 2013. An economic and technological analysis of the key factors affecting the competitiveness of electric commercial vehicles: A case study from the USA market. Transportation Research Part C: Emerging Technologies 26 135–145.

Goeke, D., M. Schneider. 2015. Routing a mixed fleet of electric and conventional vehicles. European Journal of Operational Research 245(1) 81–99.

Goel, A. 2009. Vehicle scheduling and routing with drivers' working hours. Transportation Science 43(1) 17–26.

Goel, A. 2010. Truck driver scheduling in the European Union. Transportation Science 44(4) 429–441.

Goel, A. 2012a. The Canadian minimum duration truck driver scheduling problem. Computers & Operations Research 39(10) 2359–2367.

Goel, A. 2012b. The minimum duration truck driver scheduling problem. EURO Journal on Transportation and Logistics 1(4) 285–306.

Goel, A. 2012c. A mixed integer programming formulation and effective cuts for minimising schedule durations of Australian truck drivers. Journal of Scheduling 15(6) 733–741.

Goel, A., C. Archetti, M. W. P. Savelsbergh. 2012. Truck driver scheduling in Australia. Computers & Operations Research 39(5) 1122–1132.

Goel, A., S. Irnich. 2016. An exact method for vehicle routing and truck driver scheduling problems. Transportation Science

Goel, A., L. Kok. 2012. Truck driver scheduling in the United States. Transportation Science 46(3) 317–326.

Goel, A., L.-M. Rousseau. 2012. Truck driver scheduling in Canada. Journal of Scheduling 15(6) 783–799.

Goel, A., T. Vidal. 2014. Hours of service regulations in road freight transport: An optimization-based international assessment. Transportation Science 48(3) 391–412.

Hiermann, G., J. Puchinger, S. Ropke, R. F. Hartl. 2016. The electric fleet size and mix vehicle routing problem with time windows and recharging stations. European Journal of Operational Research 252(3) 995–1018.

Hof, J., M. Schneider, D. Goeke. 2017. Solving the battery swap station location-routing problem with capacitated electric vehicles using an avns algorithm for vehicle-routing problems with intermediate stops. Transportation Research Part B: Methodological 97 102–112.

Keskin, M., B. Çatay. 2016. Partial recharge strategies for the electric vehicle routing problem with time windows. Transportation Research Part C: Emerging Technologies 65 111–127.

Koç, Ç., O. Jabali, G. Laporte. 2017. Long-haul vehicle routing and scheduling with idling options. Journal of the Operational Research Society 1–13.

Koç, Ç., T. Bektaş, O. Jabali, G. Laporte. 2016. A comparison of three idling options in long-haul truck scheduling. Transportation Research Part B: Methodological 93 631–647.

Kok, A. L., E. W. Hans, J. M. J. Schutten. 2011. Optimizing departure times in vehicle routes. European Journal of Operational Research 210(3) 579–587.

Kok, L., C. M. Meyer, H. Kopfer, J. M. J. Schutten. 2010. A dynamic programming heuristic for the vehicle routing problem with time windows and European Community social legislation. Transportation Science 44(4) 442–454.

Montoya, A., C. Guret, J. E. Mendoza, J. G. Villegas. 2017. The electric vehicle routing problem with nonlinear charging function. Transportation Research Part B: Methodological. In Press.

Pelletier, S., O. Jabali, G. Laporte. 2016. 50th Anniversary invited article–Goods distribution with electric vehicles: Review and research perspectives. Transportation Science 50(1) 3–22.

Pelletier, S., O. Jabali, G. Laporte, M. Veneroni. 2017. Battery degradation and behaviour for electric vehicles: Review and numerical analyses of several models. Transportation Research Part B: Methodological. In Press.

Pisinger, D., S. Ropke. 2007. A general heuristic for vehicle routing problems. Computers & Operations Research 34(8) 2403–2435.

Prescott-Gagnon, E., G. Desaulniers, M. Drexl, L.-M. Rousseau. 2010. European driver rules in vehicle routing with time windows. Transportation Science 44(4) 455–473.

Rancourt, M.-E., J.-F. Cordeau, G. Laporte. 2013. Long-haul vehicle routing and scheduling with working hour rules. Transportation Science 47(1) 81–107.

Roberti, R., M. Wen. 2016. The electric traveling salesman problem with time windows. Transportation Research Part E: Logistics and Transportation Review 89 32–52.

Schiffer, M., P. Klein, M. Schneider, G. Walther. 2017. A solution framework for a class of vehicle routing problems with intermediate stops. Working Paper OM-DPO 01/2017. RWTH Aachen.

Schiffer, M., S. Stütz, G. Walther. 2016. Are ECVs breaking even? - Competitiveness of electric commercial vehicles in medium-duty logistics networks. Working Paper OM-02/2016. RWTH Aachen.

Schiffer, M., G. Walther. 2017a. An adaptive large neighborhood search for the location-routing problem with intra-route facilities. Transportation Science. Forthcomming.

Schiffer, M., G. Walther. 2017b. The electric location routing problem with time windows and partial recharging. European Journal of Operational Research 260(3) 995–1013.

Schneider, M., A. Stenger, D. Goeke. 2014. The electric vehicle-routing problem with time windows and recharging stations. Transportation Science 48(4) 500–520.

Solomon, M. M. 1987. Algorithms for the vehicle routing and scheduling problems with time window constraints. Operations Research 35(2) 254–265.

Xu, H., Z. L. Chen, S. Rajagopal, S. Arunapuram. 2003. Solving a practical pickup and delivery problem. Transportation Science 37(3) 347–364.

Yang, J., H. Sun. 2015. Battery swap station location-routing problem with capacitated electric vehicles. Computers & Operations Research 55 217–232.